

Game-Theory Based Capacity Optimization of HetNets



By

Hamnah Munir

NUST201464062MSEEC61214F

Supervisor

Dr. Syed Ali Hassan

Department of Electrical Engineering

A thesis submitted in partial fulfillment of the requirements for the degree
of Masters of Science in Electrical Engineering (MS EE)

In

School of Electrical Engineering and Computer Science,
National University of Sciences and Technology (NUST),

Islamabad, Pakistan.

(December 2016)

Approval

It is certified that the contents and form of the thesis entitled “**Game-Theory Based Capacity Optimization of HetNets**” submitted by Hamnah Munir have been found satisfactory for the requirement of the degree.

Advisor: Dr. Syed Ali Hassan

Signature: _____

Date: _____

Committee Member 1: Dr. Sajid Saleem

Signature: _____

Date: _____

Committee Member 2: Dr. Fahd Ahmed Khan

Signature: _____

Date: _____

Committee Member 3: Dr. Rizwan Ahmad

Signature: _____

Date: _____

Abstract

For the past few years, 5G heterogeneous networks (HetNets) have gain phenomenal attention in the wireless industry. Millimeter wave (mmWave) technology integrated with HetNets has emerged as a new wave to overcome the thirst for higher data rates and severe shortage of spectrum. In this thesis, we analyze the performance of HetNets exploiting various 5G technologies including mmWave communication, user-centricity and dual-slope path loss model. We propose a hierarchical framework for the optimal resource allocation on the uplink of a heterogeneous network and optimize the access policy of the small cells. The proposed approach allows users to decide their connectivity between the small cell base stations (BSs) and the macrocell base station (MBS) with the goal of maximizing their rates and the overall network performance. This network-assisted user-centric approach distributes intelligence and control to the users; thereby, reducing the monitoring complexity associated with centralized control. This model is further integrated with mmWave technology to form a hybrid HetNet exploiting both microwave (μW) and mmWave frequency bands and formulate a two layer game theoretic framework to maximize the energy efficiency (EE) while optimizing the network resources. It ensures energy efficient user association method subject

to the minimum rate and maximum transmission power constraints by using dual decomposition approach. Next section focuses on the impact of dual slope path loss model on the user association. Currently, the user association techniques are under the influence of single slope path loss model. The densification of networks and irregular cell patterns have increased the variations in both the link distances and interferences; making single slope path loss models less accurate. We study multi-slope path loss model, with the focus on dual-slope, and proposes a user association scheme on the downlink of a HetNet. Simulations are performed to validate the theoretical results.

Dedication

I dedicate this thesis to my parents and teachers.

Certificate of Originality

I hereby declare that this submission is my own work and to the best of my knowledge it contains no materials previously published or written by another person, nor material which to a substantial extent has been accepted for the award of any degree or diploma at NUST SEECS or at any other educational institute, except where due acknowledgement has been made in the thesis. Any contribution made to the research by others, with whom I have worked at NUST SEECS or elsewhere, is explicitly acknowledged in the thesis.

I also declare that the intellectual content of this thesis is the product of my own work, except for the assistance from others in the project's design and conception or in style, presentation and linguistics which has been acknowledged.

Author Name: Hamnah Munir

Signature: _____

Acknowledgment

First and foremost, I would like to thank Allah Almighty for giving me the opportunity, determination and courage to complete my research. Nothing could have been possible without His blessings.

I would like to express my sincere gratitude to my advisor, Dr. Syed Ali Hassan, without whom not a single page of the thesis would have been possible. I have been extremely fortunate to work under his supervision. His consistency and valuable guidance kept me going throughout this journey for which I am eternally grateful to him. I will never forget his quick feedback and constructive comments which were really inspiring and helpful. He has set a great model for me to follow on the road of becoming a good researcher.

I, also, thank our long-term collaborator, Dr. Haris Pervaiz, whom I see as my other academic adviser. I am really grateful for his enormous help and guidance whenever I reached out to him. I will always remember how he hesitated on my poorly crafted work and helped me to improve it and how he stayed up with us before submission deadlines. I sincerely appreciate his contribution of time and guidance.

I would also like to thank all my lab mates for being amazing colleagues.

Finally, I give special thanks to my incredible parents for their tireless

efforts and guidance at every stage of my personal and academic life. I dedicate this thesis to my parents. Thank you for your endless support and unconditional confidence in me.

Table of Contents

1	Introduction	1
1.1	5G Technologies	1
1.2	Thesis Contribution	2
1.3	Thesis Organization	3
2	Background and Literature Review	5
2.1	Heterogeneous Networks	5
2.2	Millimeter Wave Technology	7
2.3	User-Centric Approaches	8
2.4	Multi-slope Path Loss Model	9
3	5G HetNets Exploiting User-centric Approaches	11
3.1	System Model	12
3.1.1	Proposed Algorithm	17
3.2	Simulation Results	20
4	5G Hybrid HetNets Exploiting mmWave Capabilities	25
4.1	System Model	26
4.2	Problem Formulation	30

<i>TABLE OF CONTENTS</i>	ix
4.3 Simulation Results	35
5 5G HetNets Exploiting Multi-Slope Path Loss Model	40
5.1 System Model	41
5.1.1 Path Loss Models	42
5.1.2 User Association	43
5.2 Simulation Results	46
6 Conclusions	54

List of Figures

1.1	A heterogeneous network.	2
2.1	A HetNet with different access policies of the FAPs.	7
2.2	Frequency Spectrum.	8
3.1	A heterogeneous network with femtocells overlaid on a macrocell.	13
3.2	Sum-rate of an all closed, optimized network-centric and proposed optimised user centric schemes for varying number of FAPs and N=7	22
3.3	Outage probability of an all closed, optimized network-centric and proposed optimised user centric schemes for varying number of FAPs with N=7.	22
3.4	Sum-rate of an all closed, optimized network-centric and proposed optimised user centric schemes vs the minimum rate requirement for N=12 and M=10 with outage (shown in % at the top of each bar).	23
3.5	Number of FAPs playing open access versus the varying number of FAPs.	23

4.1	A heterogeneous network with femtocells overlaid on a macrocell.	27
4.2	Sum-rate of a hybrid HetNet and all-UHF HetNet with and without power control with varying number of FAPs for $N=100$ and $F=5$.	37
4.3	Energy Efficiency of a hybrid HetNet and all-UHF HetNet with and without power control with varying number of FAPs for $N=100$ and $F=5$.	37
4.4	Energy Efficiency of a hybrid HetNet with power control for various interference threshold with varying number of FAPs for $N=100$ and $F=5$.	39
4.5	Energy Efficiency of a hybrid HetNet with power control with varying density of mmWave FAPs for $M=15$, $F=5$ and $N=100$.	39
5.1	A two-tier heterogeneous network with red circles showing the critical radius of picocell and macrocell.	41
5.2	Fraction of users connected to pico-tier when biased received power association is used across varying biasing factor of pico-tier, θ_2 , for $N = 100$, $M = 4$, $\theta_1 = 0$ dB, $[\alpha_1, \alpha_2](\text{Macro-tier}) = [4, 5]$ and $[\alpha_1, \alpha_2](\text{Pico-tier}) = [3, 4]$.	47
5.3	Fraction of users connected to pico-tier when biased received power association is used across varying biasing factor of pico-tier, θ_2 , for $N = 100$, $M = 4$, $\theta_1 = 0$ dB, $[\alpha_1, \alpha_2](\text{Macro-tier}) = [3, 4]$ and $[\alpha_1, \alpha_2](\text{Pico-tier}) = [2, 4]$.	49

5.4 Fraction of users connected to pico-tier when biased received power association is used across varying biasing factor of pico-tier, θ_2 , for $N = 100$, $M = 4$, $\theta_1 = 0$ dB, $[\alpha_1, \alpha_2](\text{Macro-tier}) = [3, 4]$ and $[\alpha_1, \alpha_2](\text{Pico-tier}) = [2, 4]$ 50

5.5 Fraction of users connected to pico-tier when path loss association is used across varying density of PBSs for $N = 100$, $\theta_1 = \theta_2 = 0$ dB, $[\alpha_1, \alpha_2](\text{Macro-tier}) = [4, 5]$ and $[\alpha_1, \alpha_2](\text{Pico-tier}) = [3, 4]$ 51

5.6 Fraction of users connected to pico-tier when association is done based on biased maximum rate across varying pico-tier bias factor, θ_2 , for $N = 50$, $M = 4$, $\theta_1 = 0$ dB, $[\alpha_1, \alpha_2](\text{Macro-tier}) = [4, 5]$ and $[\alpha_1, \alpha_2](\text{Pico-tier}) = [3, 4]$ 51

5.7 Fraction of users connected to pico-tier when biased received power association is used across varying critical radius of picocell for $N = 100$, $M = 4$, $\theta_1 = \theta_2 = 0$ dB 52

List of Tables

4.1	Simulation Parameters.	37
5.1	Parameter Notation.	44
5.2	Simulation Parameters.	47

Chapter 1

Introduction

This chapter presents a brief introduction about fifth generation (5G) networks. After that, thesis contribution is presented and then, thesis organization concludes this chapter.

1.1 5G Technologies

The future of connectivity, in the next generation of mobile networks, is extending beyond connecting people- it's about connecting everything. In this regard, 5G will bring the today's generation style of 4G networks into the new era of wireless communication with an addition of a globally standardized radio access technology.

In this thesis, we discuss the technologies like ultra-dense networks (UDN), millimeter wave (mmWave) technologies, user-centric approaches and multi-slope path loss model. The UDN allows the fusion of technologies, frequency bands, diverse cell sizes and network architectures to handle the drastic pro-

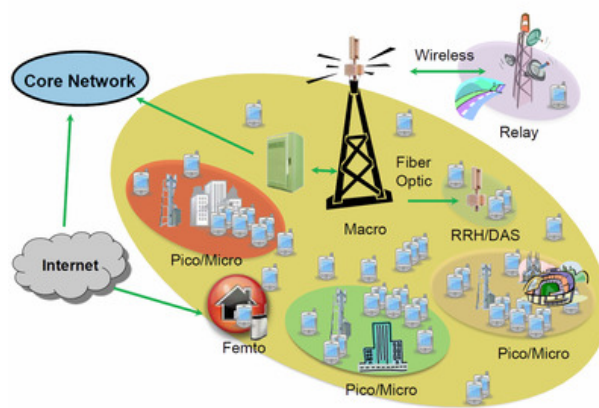


Figure 1.1: A heterogeneous network.

liferation of data traffic and expanded cell coverage. This UDN paradigm has paved the way of bandwidth expansion by enabling the coalition of frequency bands. The integration of mmWave frequency band with microwave frequency band has stolen the limelight as a promising solution to provide ubiquitous high data rates to the users. This flexibility of air-interfaces and increasing network scalability has made the centralized control a challenging task. User-centric approaches have come to aid to overcome the complexity of centralized monitoring and in realizing trenchant users' preferences and requirements. This article attempts to provide insights on advantages and challenges associated with these technologies and proposes framework to realize the importance of these technologies.

1.2 Thesis Contribution

The main contributions of this paper can be listed as:

- This thesis models the preferred access policy of the small cells among

open, closed and hybrid. The main focus is to analyze the conflicting interests of the small cell base stations (BSs). This selection of access policy on the uplink is a tradeoff between interference avoidance and saving resources and has a significant impact on the performance of the network.

- It further implements the user-centric approach to overcome the centralized monitoring complexity and compares it with network-centric approach.
- We propose a hybrid heterogeneous network (HetNet) scheme exploiting the mmWave frequency band which improves the sum-rate and energy efficiency (EE) in comparison to the scenario where all the networks operate at sub-6 GHz frequency band using Lagrangian Dual Decomposition approach.
- The user association and load balancing is analyzed and we prove that the multi-slope path loss model outperforms the conventional single slope path loss model. The dual slope path loss model lead to steering of users to nearby small cells, thus off loading the traffic from macrocell base station.

1.3 Thesis Organization

The rest of the thesis is organized as follows: Chapter 2 presents the background and existing literature on the future technologies of 5G wireless networks. In chapter 3, we formulate a framework to maximize the data rates in

HetNets, in a user-centric fashion. Chapter 4 presents a HetNet coupled with mmWave technology and proposes a framework for energy efficient resource allocation in a hybrid HetNet. Chapter 5 introduces the multi-slope path loss model and analyzes its impact on user association in HetNets. Chapter 6 generalizes the conclusion drawn from the above frameworks along with the concluding remarks.

Chapter 2

Background and Literature

Review

This chapter presents the background and literature review on the future technologies of next generation mobile network. It discusses the key technologies of 5G wireless networks including small cell networks, higher frequency bands, user-centric approaches and multi-slope path loss models. It also discusses the capabilities of these technologies and their impact on 5G mobile communications.

2.1 Heterogeneous Networks

With the drastic increase in wireless data traffic, the demand for higher data rates has become a key necessity for the next generation mobile network. To manage this staggering growth of wireless data traffic, HetNets have drawn tremendous attention in the next generation mobile systems. Heterogeneity

in the wireless environment allows low power BSs, deployed in small cells of diverse sizes overlaid on a macrocell, to operate at different frequency bands that makes an efficient use of the radio resources [1, 2]. This overlay deployment of low power BSs, to complement the conventional cellular network, has a great potential to cope with the drastic proliferation of wireless data traffic by allowing the fusion of technologies, frequency bands, diverse cell sizes and network architectures [3]. They ensure significant enhancement in the overall network performance that include high data rates and expanded cell coverage [4, 5]. Nevertheless, these perks are accompanied by new technical challenges namely hardware expenses, interference management, user association, load balancing, radio resource management, energy efficiency along with the others [6–8, 10, 11, 46].

The deployment of small cells (microcells, picocells and femtocells) helps in increasing the sum-rate of the network but makes interference and centralized control a challenging issue [12]. A considerable amount of literature is available to address this concern of interference as seen in [14] and the references therein. The concern related to centralized control can be overcome using user-centric approaches.

The femtocell access points (FAPs) can operate in different modes: closed, open and hybrid [15], as shown in Fig .2.1. In closed access scheme, resource sharing is not allowed and FAPs dedicate all of their resources to their home subscribers. Whereas, in open access scheme, FAPs share their resources with the macrocell users in order to avoid interference and to enhance the network performance. The hybrid access policy puts a limit on the resource allocation to macrocell users [16]. The selection of access policy on the uplink

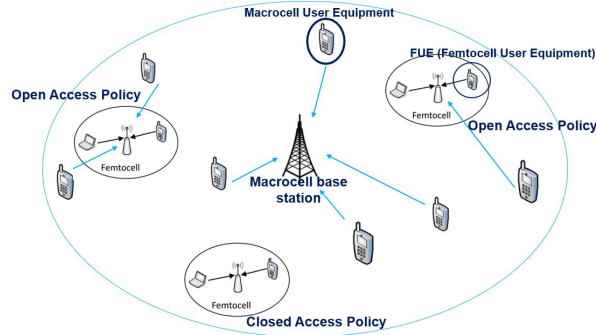


Figure 2.1: A HetNet with different access policies of the FAPs.

is a tradeoff between interference avoidance and saving resources and has a significant impact on the performance of the network. Several existing works used the game theoretical models to optimize the performance of femtocells in the HetNets [17].

2.2 Millimeter Wave Technology

The fusion of frequency bands in HetNets has paved the way of bandwidth expansion, by integrating mmWave bands into the current cellular network, to overcome the problem of capacity shortage. MmWave technology represents the next advance in the wireless industry [18, 19]. This fragment of spectrum, ranging from 30 – 300 GHz, has stolen the limelight as a promising solution to provide ubiquitous high data rates to the users [21, 22, 37]. While improving network performance, it faces many challenges including hardware expenses, non-line-of-sight (NLOS) signal range and large distance connections [23]. However, with the help of highly directional antennas and beamforming, significant signal strength can be achieved within a range of about 150-200 meters. Significant advancements have also been seen in the

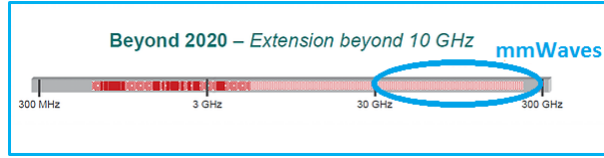


Figure 2.2: Frequency Spectrum.

manufacturing of low cost mmWave hardware. The coalition of mmWave small cells with conventional microwave (μ W) network in a hybrid HetNets will resolve the hardware problem along with bolstering network capacity and improving the mobile user experience [24, 25].

2.3 User-Centric Approaches

This flexibility of air-interfaces and increasing network scalability has made the centralized control a challenging task. In this regard, user-centric schemes have emerged as a potential solution to overcome the complexity of centralized monitoring by authorizing users to make decisions at less computational complexity [26]. Traditional cellular networks are inherited with network-centric approaches, which usually falls short in providing trenchant user requirements. User-centric approaches have come to aid in realizing users' preferences and requirements [27, 28]. In a user-centric approach, user is on top of all that makes decision with or without network-assistance. It requires less computational complexity whereas network-centric scheme can make more informed decisions at the cost of monitoring overhead. The amalgamation of user-centric approach-which focuses on the interest of users and network-centric approach-which focuses on the interest of network, can generate interesting results [29].

2.4 Multi-slope Path Loss Model

Recently, numerous studies have focused on the mixed deployment using macrocell and distributed small cells, which have shown significant results to get higher throughput gains in dense networks. To manage the high user density and to increase the capacity, it is desirable to shift the traffic load from macrocell to small cells. HetNets, consisting of small cells with smaller coverage range, allow small cell BSs to communicate at lower powers which limits the fraction of users connected to them, resulting in congestion at the macro-tier. Different load balancing techniques are studied to offload the traffic from macro-tier [30, 31]. One promising way to resolve this issue is through static cell biasing that allows users to offload to small cells using a biased measured signal. This suboptimum offloading technique is known as *cell range expansion*. However, the traffic demand in hot spots in the dense networks often varies with time, which calls to dynamically adjust the biases, resulting in enhanced load balancing gains [32, 33].

Most of the existing literature uses single slope path loss model to represent the path loss over the entire coverage range. While the single slope model is easy to study and analyze, it sometimes characterize the network unrealistically. This performance degradation occurs as this model does not capture the dependence of path loss exponent on the link distance perfectly [34]. However, in the most recent works, this trend is shifted more towards dual slope path loss model. This migration is influenced by the network densification [35], irregular cell patterns [36] and recent work on millimeter wave (mmWave) communications because of highly intermittent links [37]. The

mmWave spectrum, ranging from 10-300 GHz, improves the network performance but faces many challenges including sensitivity to blocking. Dual slope path loss model has a great potential to better approximate the line of sight (LOS) and NLOS links, in mmWave systems, using different path loss exponents.

Multi-slope models apply different slopes for different link distances, which result in improved performance for dense networks. This model was first studied for LOS environment for free space reference distance model in [38] and for indoor scenario in [39]. In [40], dual slope model has been proposed to reduce the root mean square (RMS) error between local mean path loss samples and the path loss model, for NLOS environment. In [41], coverage probability and network throughput has been analyzed and studied under multi-slope path loss model on a downlink of a cellular network. In [42], dual slope path loss models are used to study the coverage probability with varying user density. The authors in [43] extended this work to user association in HetNets using dual slope path loss model. It further analyzed the impact of biasing and uplink/downlink decoupling with dual slope model on user association.

Chapter 3

5G HetNets Exploiting User-centric Approaches

In this chapter, we present a hierarchical game theoretical framework consisting of two sub-games for resource allocation to optimize the sum-rate of a heterogeneous network. This scheme starts by modeling the FAPs preferred access policies to optimize the performance of their registered users in the first game, given the state of the network. The main focus of this part is to analyze the conflicting interests of the FAPs in the selection of their optimized access policies. The second game uses user-centric approach by allowing macrocell users to finalize their association in order to maximize their interest while keeping in view the network performance. To solve this hierarchical game framework, we devise a distributed scheme which always reaches a pure strategy Nash equilibrium (PSNE). The coalition of two games optimises the data rates for macrocell users and femtocell users, at the expense of increased complexity of the game problem. Simulations have shown

that this proposed scheme outperforms the network-centric scheme by a huge margin.

3.1 System Model

Consider the uplink of a single cell HetNet having M femtocell access points (*FAPs*) overlaid on a macrocell, as shown fig. in 4.1, having N macrocell user equipments (*MUEs*). Let $\mathbf{M} = \{1, 2, \dots, M\}$ be the set of FAPs and $\mathbf{N} = \{1, 2, \dots, N\}$ be the set of macrocell users. We assume that a single femtocell user equipment (*FUE*) is connected to each FAP. The system bandwidth, B , is divided among FAPs in such a way that each FAP has K subcarriers available, where $K = B/M$. This implies that the FUEs do not create interference on the uplink to other FAPs as different FAPs are allocated orthogonal bands using OFDMA. The same bandwidth, B , is also used by the macro base station (*MBS*), where each MUE gets L subcarriers ($L = B/N$), which introduces cross-tier interference between the femtocells and the macrocell.

In this paper, we assume a Rayleigh fading channel with path loss. The channel between the m^{th} FAP and n^{th} MUE on k^{th} subcarrier is denoted by $h_{nm}[k]$, whereas the distance between them is denoted by d_{nm} . Similarly, the channel between the FUE and its corresponding FAP on the k^{th} subcarrier be $h_{0m}[k]$ and the distance between them is symbolized by d_{0m} . Assume the channel between n^{th} MUE and MBS on l^{th} subcarrier to be $h_{nb}[l]$ and the distance between them be d_{nb} . The channel between the FUE of m^{th} FAP and MBS is denoted by $h_{mb}[l]$ separated by the distance d_{mb} . The transmit

power of n^{th} MUE is signified by P_n and transmit power of each FUE by P_0 . A Gaussian noise with zero mean and σ^2 variance is added to all subcarriers at all FAPs and MBS.

The signal-to-interference-plus-noise ratio (SINR) for the FUE at the m^{th} FAP is given by

$$SINR_m[k] = \frac{\mu_m[k]}{\sigma^2[k] + \sum_{n=1}^N (\prod_{i=1}^M \mathbb{1}_{\rho_n^i[k]=0}) \mu_n^m[k]}, \quad (3.1)$$

and the SINR for n^{th} MUE at m^{th} FAP is given by

$$SINR_{n,m}[k] = \frac{[1 - (\prod_{i=1}^M \mathbb{1}_{\rho_n^i[k]=0})] \mu_n^m[k]}{\sigma^2[k] + \sum_{n=1}^N (\prod_{i=1}^M \mathbb{1}_{\rho_n^i[k]=0}) \mu_n^m[k]}, \quad (3.2)$$

where $\mu_m[k] = (h_{0m}[k])^2 P_0 W (d_{0m})^{-\beta}$ is the received power from FUE at m^{th} FAP on k^{th} subcarrier and $\mu_n^m[k] = (h_{nm}[k])^2 P_n (d_{nm})^{-\alpha}$ is the received power from n^{th} MUE at m^{th} FAP on the k^{th} subcarrier. The value $W < 1$ is the wall penetration loss, α and β are the path loss exponents.

Let $\rho_n^m[k] \in \{0, 1\}$ signifies the connection of n^{th} MUE to m^{th} FAP on the k^{th} subcarrier. The connectivity between n^{th} MUE and m^{th} FAP on the k^{th} subcarrier occurs when $\delta_n^m[k] = 1$ and vice versa. The indicator function, $\mathbb{1}$,

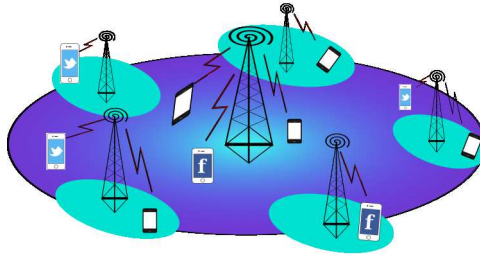


Figure 3.1: A heterogeneous network with femtocells overlaid on a macrocell.

is defined as

$$\mathbb{1}_{\{x\}} = \begin{cases} 1 & x = 0 \\ 0 & x = 1 \end{cases}.$$

Here SINR of the n^{th} MUE at MBS is expressed as

$$SINR_{n,b}[l] = \frac{(\prod_{i=1}^M \mathbb{1}_{\rho_n^i[l]=0})\mu_n^b[l]}{\sigma^2[l] + \sum_{n=1}^N [1 - (\prod_{i=1}^M \mathbb{1}_{\rho_n^i[l]=0})]\mu_n^b[l] + \sum_{m=1}^M \mu_m^b[l]}, \quad (3.3)$$

where $\mu_n^b[l] = (h_{nb}[l])^2 P_n (d_{nb})^{-\alpha}$ is the received power at MBS from n^{th} MUEs on l^{th} subcarrier and $\mu_m^b[l] = (h_{mb}[l])^2 P_0 (d_{mb})^{-\alpha}$ is the received power at MBS from FUE of m^{th} FAP on l^{th} subcarrier.

In our proposed approach, a hierarchical game consisting of two non-cooperative games is being played in a sequential order. In the first game, each FAP decides among open, closed and hybrid policy. Open access policy allows MUEs to connect to FAPs to reduce interference at the expense of resources. The closed access saves resources at the price of interference, whereas the hybrid policy is the trade off between interference and the cost of resources. This decision of FAPs depends on the interference from the MUEs and also on the choice of other FAPs, e.g., multiple FAPs cannot serve the same user as it would end up in resource wastage. Thus, the FAPs form a non-cooperative game with the goal of maximizing the rate of their FUEs by deciding its access policies. The strategy vector of FAP is the fraction of frequency band allocated to each MUE and utility function is the rate of its FUE, which can be written as

$$\tilde{v}_m(\boldsymbol{\rho}_m, \boldsymbol{\rho}_{-m}) = \sum_{k=1}^K \left(\prod_{i=1}^M \mathbb{1}_{\rho_n^i[k]=0} \right) \log(1 + SINR_m[k]), \quad (3.4)$$

where $\boldsymbol{\rho}_m = [\rho_{1,m}[1], \dots, \rho_{N,m}[1], \rho_{1,m}[2], \dots, \rho_{N,m}[K]]^T$ is strategy vector of m -th FAP, $\boldsymbol{\rho}_{-m} = [\boldsymbol{\rho}_1^T, \dots, \boldsymbol{\rho}_{m-1}^T, \boldsymbol{\rho}_{m+1}^T, \dots, \boldsymbol{\rho}_M^T]^T$ shows the strategy vector of other FAPs and $[\cdot]^T$ denotes the transpose operator.

In the other game, the MUEs re-evaluate their connectivity obtained from previous game, forming another non-cooperative game with the goal of maximizing their rates without affecting the overall network performance. The strategy vectors of the MUEs are the fraction of band allocated to them by FAPs and MBS and the utilities are their rates. The utility function can be expressed as

$$\begin{aligned} \tilde{v}_n(\boldsymbol{\rho}_n, \boldsymbol{\rho}_{-n}) = & \sum_{k=1}^K [1 - (\prod_{i=1}^M \mathbb{1}_{\rho_n^i[k]=0})] \log(1 + SINR_m[k]) + \\ & \sum_{l=1}^L [(\prod_{i=1}^M \mathbb{1}_{\rho_n^i[l]=0})] \log(1 + SINR_b[l]), \end{aligned} \quad (3.5)$$

where $\boldsymbol{\rho}_n = [\rho_{1,n}[1], \dots, \rho_{M,n}[1], \rho_{1,n}[2], \dots, \rho_{M,n}[2], \dots, \rho_{M,n}[K], \rho_{b,n}[1], \dots, \rho_{b,n}[L]]^T$ is strategy vector of n^{th} MUE and $\boldsymbol{\rho}_{-n} = [\boldsymbol{\rho}_1^T, \dots, \boldsymbol{\rho}_{n-1}^T, \boldsymbol{\rho}_{n+1}^T, \dots, \boldsymbol{\rho}_N^T]^T$ includes the strategy vectors of other MUEs.

The rate obtained by the MUE should not be less than a minimum acceptable rate, R_{\min} , which is fixed for all MUEs in the network. In case of connectivity between m^{th} FAP and n^{th} MUE, this constraint is given by

$$(1 - \prod_{i=1}^M \mathbb{1}_{\rho_n^i[k]=0}) R_{\min} \leq \sum_{k=1}^K \rho_n^m[k] \log(1 + \frac{\mu_n^m[k]}{\sigma^2[k] + \sum_{n=1}^N (\prod_{i=1}^M \mathbb{1}_{\rho_n^i[k]=0}) \mu_n^m[k]}), \quad (3.6)$$

and for n^{th} MUE connectivity with MBS, this constraint is written as

$$\left(\prod_{i=1}^M \mathbb{1}_{\rho_n^i[l]=1}\right) R_{\min} \leq \sum_{l=1}^L \rho_n^b[l] \log\left(1 + \frac{\mu_n^b[l]}{\sigma^2[l] + \sum_{m=1}^M \mu_m^b[l] + \sum_{n=1}^N [1 - (\prod_{i=1}^M \mathbb{1}_{\rho_n^i[l]=0})] \mu_n^b[l]}\right). \quad (3.7)$$

Now the strategy space for m^{th} FAP in the first phase is given as

$$\tilde{\chi}_m = \{\boldsymbol{\rho}_m[k] \in (0, 1)^{NK} : \sum_{n=1}^N \rho_n^m[k] \leq 1\}. \quad (3.8)$$

The above constraint makes sure that not more than one MUE can be connected to m^{th} FAP on k^{th} subcarrier. For given strategy vectors of other FAPs, we can define the optimization problem solved by m^{th} FAP as

$$\max_{\boldsymbol{\rho}_m \in \tilde{\chi}_m} (\boldsymbol{\rho}_m, \boldsymbol{\rho}_{-m}). \quad (3.9)$$

Strategy space of n^{th} MUE for the second game is

$$\tilde{\chi}_n = \{\boldsymbol{\rho}_n[l] \in (0, 1)^{(M+1)L} : (\rho_n^m[l] + \rho_n^b[l]) \leq 1\}. \quad (3.10)$$

This constraint ensures that the MUE cannot be connected to a FAP and MBS simultaneously. We can thus write the optimization problem as

$$\max_{\boldsymbol{\rho}_n \in \tilde{\chi}_n} (\boldsymbol{\rho}_n, \boldsymbol{\rho}_{-n}). \quad (3.11)$$

We have solved the above games using Nash equilibrium. Nash equilibrium

is attained by $(\mathbf{x}^*_i, \mathbf{x}^*_{-i})$ when

$$\tilde{f}_i(\mathbf{x}^*_i, \mathbf{x}^*_{-i}) \geq \tilde{f}_i(x_i, \mathbf{x}^*_{-i}); \forall x_i \in \tilde{\chi}_i, \quad (3.12)$$

where x_i represents the strategy vector of i^{th} player with the utility function f_i .

3.1.1 Proposed Algorithm

We propose a distributed solution, which aims at maximizing the rate given to the users by optimizing the trade off between interference and the resources. The algorithm always reaches a pure strategy Nash equilibrium (PSNE) while achieving stable action profiles. It starts by allowing FAPs to select their strategies while knowing the strategies of other FAPs at any point in time, which is done using a parallel update technique. Using the information of other FAPs from the $(i - 1)^{th}$ iteration, each FAP selects its own strategy at the i^{th} iteration. The first step is to form an initial strategy vector λ_0 , without seeking equilibrium. In this vector, optimal resources are allocated to all MUE while satisfying (3.6) using

$$\lambda_n^m = \frac{R_{\min}}{\log(1 + \frac{\mu_n^m}{\sigma^2})}. \quad (3.13)$$

After that, each FAP explores the favorable set of MUEs (N_m^i) in each iteration, given the strategies of other FAPs from $(i - 1)^{th}$ iteration. The selection of N_m^i (N_m^i can be empty) is done in order to maximize the rates of FUEs (utility function of the FAPs). In case of open access, each FAP

needs to optimize the selection of N_m^i by checking the utility from servicing a certain set of MUEs. To avoid complexity, the FAP could find optimal set of MUEs with the help of greedy algorithm as used in [44] rather than testing all possible combinations of MUEs. Greedy algorithm helps FAPs by finding highly interfering MUEs. Each iteration ends with the assurance that multiple FAPs are not allocating resources to a single MUE as it would result in the waste of resources. The connectivity between FAPs and MUEs ensures the best interest of the users of FAPs. These iterations continues until convergence, which can also be achieved using other schemes, such as in [49].

Algorithm 3.1

Find λ_0 .

REPEAT

for $m = 1$ **to** M **do**

Find N_m^i , given ρ_{-m} from $(i - 1)$.

Allocate sub-band $\forall n \in N_m^i$.

Discard association $\forall n \notin N_m^i$.

end for

if $\sum_{m=1}^M \rho_{n,i}^m[k] > 1$ **then**

Set $\rho_{n,m}[k] = \rho_{m,n}^*[k]$ for which $\mu_n^m[k]$ is max.

Set $\rho_{n,-m}[k] = 0$.

end if

Repeat till PSNE is achieved.

END

Find data rates for FUEs at FAPs.

Find data rates for MUEs at open FAPs and MBS.

$N^* = N_1^i \cup N_2^i \cup \dots \cup N_M^i$

$c_1 =$ Sum-rate when the n^{th} MUE is connected to the MBS.

$c_2 =$ Sum-rate when the n^{th} MUE is connected to the m^{th} FAP.

REPEAT

for $n = 1$ to N^* **do**

if (Rate from MBS > Rate from m^{th} FAP) **then**

if ($c_1 > c_2$) & (Rate from MBS > R_{\min}) **then**

Set $\rho_{b,n}[l] = \rho_{b,n}^*[l]$ & $\rho_{m,n}[l] = 0$.

else

Set $\rho_{m,n}[l] = \rho_{m,n}^*[l]$ & $\rho_{b,n}[l] = 0$.

end if

else

Set $\rho_{m,n}[l] = \rho_{m,n}^*[l]$ & $\rho_{b,n}[l] = 0$.

end if

end for

Repeat till PSNE is achieved.

END

for $n = 1$ to $N^{*'}$ **do**

if (Rate from MBS < R_{\min}) **then**

Set $\rho_{b,n}[l] = 0$.

end if

end for

After maximizing the rates of FUEs, MUEs play the next game to maximize their rates using user-centric approach. MUEs which are connected to FAPs, as a result of previous game, examine the rates they are getting from FAP and MBS. MUEs stay connected to FAPs if the utility is greater for that case. If the rate that the MUE is getting from the MBS is greater, then the sum-rate is calculated for both cases with MUE connected to MBS and with FAP. Each MUE opts for the case where system is not affected and it gets the rate greater than a defined threshold of R_{\min} . If the constraint of R_{\min} is

not met, the particular MUE goes into outage. At the end of this game, each MUE ensures that it is not connected to FAP and MBS simultaneously, thus saving resources. The above steps are continued until all MUEs, which were previously connected to FAPs, finalize their strategies in the best interest of the network and themselves.

3.2 Simulation Results

In this section, we present the numerical results of our proposed algorithm with respect to various network parameters. We consider a cell of 1000m radius where the FAPs and the MUEs are uniformly scattered over the area. The FUEs and the MUEs are assured to have same transmit power of 0.2 W. The path loss exponent $\alpha = 2$, $\beta = 2.5$ and the wall penetration loss $W = 0.5$ is assigned. The distance between each FAP and its corresponding FUE is $1m$. It is assumed for simplicity that each FAP has one FUE. The noise variance is set to $\sigma^2 = 10^{-14}$. The system bandwidth, $B = 10\text{MHz}$ and the minimum acceptable data rate for the MUEs is 500kbps unless stated otherwise.

We have compared our proposed scheme with two other schemes. The first comparison is done with an all-closed access policy scheme, where all the FAPs have adopted a closed access that results in connecting all the MUEs to the MBS. On the other hand, the second comparison is with the network-centric optimized scheme. This scheme allows FAPs and MBS to decide the connectivity of their users. Hence the central entity reserves all the control. In our proposed scheme, we have merged the network-centric

and user-centric approach by spreading the control and intelligence in the network rather than keeping it to the central entity. This user-centric scheme not only overtakes the network-centric scheme in terms of performance but also offloads the complex computation from MBS and distributes it to the network, thus requiring less computational and monitoring complexity.

Fig. 3.2 shows a comparison of the achieved sum-rate of the proposed scheme with closed access and network-centric optimized schemes. We can see that as M increases, the sum-rate increases for the proposed scheme. This is because the likelihood of the FAPs playing open access increases with an increase in the number of FAPs, which in return service the interfering MUEs; thus improving the performance of the system and decreasing the outage probability. The same trend of sum-rate is followed in the network-centric scheme but user-centric scheme yields a significant improvement in terms of utilities. In the case of all closed access scheme, the sum-rate almost remains constant, although the number of FAPs increases. This is due to the fact that as the density of FAPs increases in the network, the MUEs appear closer to them resulting in increased interference. This, in turn, decreases the data rates of the FUEs and also forces the MUEs to go in outage as seen in Fig. 3.3. The outage probability trend is same for both user-centric and network-centric schemes as demonstrated in Fig. 3.3, however, the proposed approach performs better in terms of achieved data rate. Thus, we can say that our scheme is as fair as network-centric though more capacity oriented.

Fig. 3.4 shows the comparison of sum-rate for an all closed scheme, optimized network-centric scheme and proposed scheme against different minimum rate requirements. The percentage of users in outage for the proposed

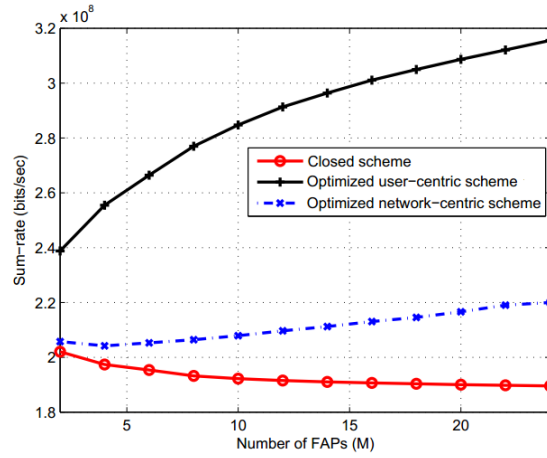


Figure 3.2: Sum-rate of an all closed, optimized network-centric and proposed optimised user-centric schemes for varying number of FAPs and $N=7$

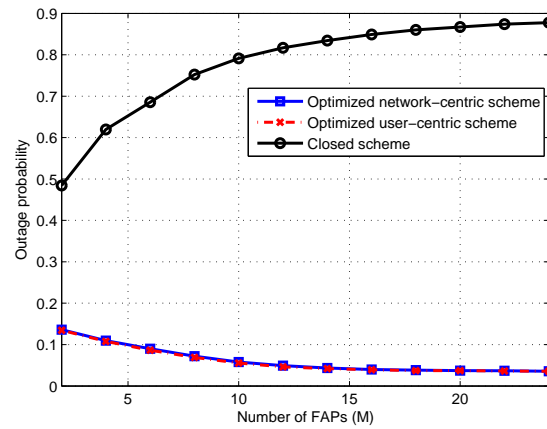


Figure 3.3: Outage probability of an all closed, optimized network-centric and proposed optimised user-centric schemes for varying number of FAPs with $N=7$.

and network-centric schemes is same although the sum-rate for proposed scheme is better as described earlier. This difference in sum-rate decreases as the minimum required rate increases because the condition of R_{\min} is not satisfied and MUEs do not participate in the optimization of sum-rate. How-

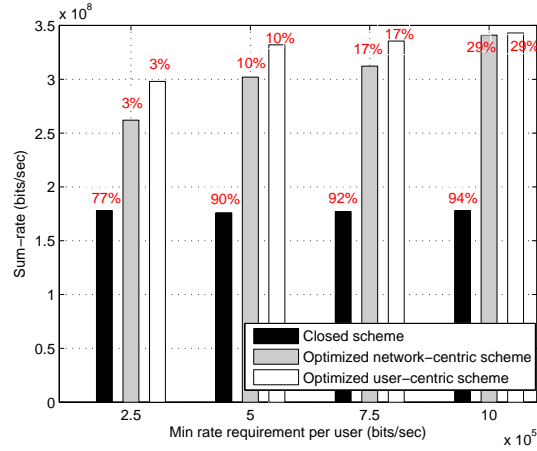


Figure 3.4: Sum-rate of an all closed, optimized network-centric and proposed optimised user centric schemes vs the minimum rate requirement for $N=12$ and $M=10$ with outage (shown in % at the top of each bar).

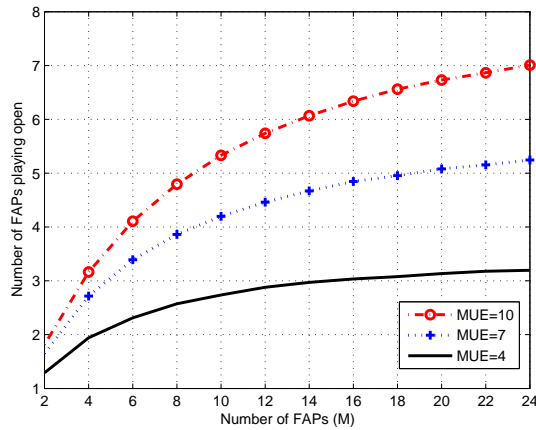


Figure 3.5: Number of FAPs playing open access versus the varying number of FAPs.

ever, for increased number of users, this difference will again prevail. In case of all closed scheme, the sum-rate remains constant while the outage percentage increases. This trends shows that for small value of minimum required rate e.g. 250kbps, lesser users are in outage while for high value of rate requirement, e.g., 1Mbps, more users are in outage, however, each serviced

user is getting four times the data rate than the previous case. Hence the overall rate attained remains the same.

In Fig. 3.5, the number of FAPs playing open access policy are shown for our proposed approach. We can see that as M increases, the number of open FAPs starts increasing to service the MUEs till it reaches a saturation point. This trend shows that as the number of FAPs start getting larger than the MUEs, additional FAPs should not play open to save their resources. We can observe that the number of FAPs playing open increases when $M \leq 6$ for a total of $N = 7$. However, for $N = 10$ this increasing trend continues for $M \leq 8$ and this number increases for $M \leq 3$ in case of $N = 4$.

Chapter 4

5G Hybrid HetNets Exploiting mmWave Capabilities

Drastic increase in the data traffic and substantial growth of network infrastructures has aggravated the concern of energy consumption [45, 46]. This challenge has made developing energy efficient system, a key necessity for the next generation mobile networks. HetNets, consisting of small cells with smaller coverage range, allows BSs and user equipments (UEs) to communicate at lower powers which results in the reduction of energy consumption and also the interference [47, 48].

In this chapter, we formulate a two layer framework for energy efficient resource allocation in a hybrid HetNet. In the first game, each femtocell access point (FAP) models its preferred access policy for both mmWave and UHF frequency bands, given the state of the network, to optimise the data rates of its home users. Then, these FAPs opt for one of these bands in the best interest of the network using a network-centric approach. To solve

this game, we devise a scheme, which always reaches a PSNE. It is then followed by the next game where MUEs finalize their association, in a user-centric fashion with network assistance, while maximizing energy efficiency (EE) considering the power and minimum rate constraints. This game is solved using Lagrangian dual decomposition approach. The performance of this hybrid HetNet is compared with the stand alone UHF networks.

4.1 System Model

Consider the uplink of a two-tier HetNet having M FAPs overlaid on a macrocell, as shown in Fig. 4.1, where a total of N macrocell user equipments (MUEs) are randomly distributed. Let $\mathbb{M} = \mathbb{M}_M \cup \mathbb{M}_U$ be the set of FAPs where \mathbb{M}_M represents the set of FAPs operating on mmWave band and \mathbb{M}_U be the set of FAPs operating on UHF band whereas $\mathbb{M}_o = \{m_o\}$ be the singleton set representing macrocell base station (MBS). Similarly, let $\mathbb{N} = \mathbb{N}_o \cup \mathbb{N}_M$ be the set of MUEs where \mathbb{N}_o be the set of MUEs connected to MBS and $\mathbb{N}_M = \bigcup_{m=1}^M \mathbb{N}_m$ be the set of MUEs connected to the m^{th} FAP. On the other hand, $\mathbb{F} = \bigcup_{m=1}^M \mathbb{F}_m$ denotes the set of femtocell user equipments (FUEs) where each $\mathbb{F}_m = \{1, 2, \dots, F\}$ is the set of FUEs connected to a single FAP. Also let $\mathbb{I} = \mathbb{N} \cup \mathbb{F}$ be the set of all the users in the network and $\mathbb{J} = \mathbb{M} \cup \mathbb{M}_o$ be the set of all the base stations in the network.

The FAPs operating on mmWave band split the bandwidth, B_m , into identical K_m sub-bands depending on the number of users connected to them. On the other hand, FAPs operating on UHF band assign entire bandwidth B consisting of K subcarriers to all connected users. The same bandwidth,

B , is also used by the MBS operating on UHF band. Hence, each MUE gets bandwidth B comprising of L subcarriers, which introduces cross-tier interference on UHF band.

The path loss models for this system are expressed by the following equations for mmWave and UHF links, respectively

$$L_{\text{mmW}}(d)[\text{dB}] = \begin{cases} b + 10\alpha_L \log(d) + \Omega_L & \text{if link is LoS} \\ b + 10\alpha_N \log(d) + \Omega_N & \text{otherwise.} \end{cases} \quad (4.1)$$

$$L_{\text{UHF}}(d)[\text{dB}] = 20 \log\left(\frac{4\pi}{\lambda_c}\right) + 10\beta \log(d) + \Psi, \quad (4.2)$$

where d is the distance in meters, Ω_L and Ω_N are zero mean log normal random variables for line-of-sight (LoS) and non-line-of-sight (NLoS) mmWave links, respectively. Ψ represents the log normal random variable in the case of UHF links. In (5.2), $b = 32.4 + 20\log(f_c)$ shows the fixed path loss for mmWave links, where f_c is the carrier frequency. Similarly in (5.1), λ_c corresponds to the carrier wavelength in case of UHF link. The path loss exponents for LoS and NLoS mmWave links are indicated by α_L and α_N , respectively, whereas the path loss exponent for UHF links is denoted by β .

To maintain the quality-of-service (QoS) requirements of the users, a

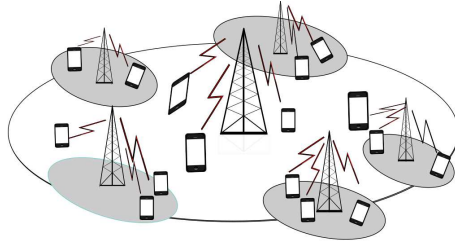


Figure 4.1: A heterogeneous network with femtocells overlaid on a macrocell.

constraint on the cross-tier interference is applied to find the optimal transmit power of the users. Let $\rho_i^j[x] \in \{0, 1\}$ denotes the connection between any i^{th} user and any j^{th} BS on any subcarrier x . In case of connectivity, $\rho_i^j[x] = 1$, otherwise $\rho_i^j[x] = 0$. Let $I[x]$ denote the interference threshold for the m^{th} BS on the x^{th} subcarrier and we have

$$\sum_{\substack{j \in \mathbb{J} \\ j \neq m}} \sum_{i \in \mathbb{I}} \rho_i^j[l] g_{ij}[l] p_i^j[l] \leq I_m[x], \quad \forall x, \quad (4.3)$$

where g_{ij} is product of the magnitude squared of the channel gain and the inverse of the path loss between the i^{th} user and the j^{th} BS and p_i^j represents the optimal transmit power of the i^{th} user with the constraint that

$$p_i \leq P_i^{\max}, \quad \forall i, \quad (4.4)$$

where P_i^{\max} is the maximum transmit power of the i^{th} user.

The received power of the i^{th} user at the j^{th} BS, separated by the distance d_{ij} , on x^{th} subcarrier is given as

$$\mu_i^j[x] = \begin{cases} \frac{p_i^j G(\theta_j) |h_{ij}[x]|^2}{L_{\text{mmW}}(d_{ij})} & \text{mmWave,} \\ \frac{p_i^j |h_{ij}[x]|^2}{L_{\text{UHF}}(d_{ij})} & \text{UHF,} \end{cases} \quad (4.5)$$

where p_i^j is the transmit power and $h_{ij}[x]$ represents the channel. $G(\cdot)$ is the antenna gain and θ_j is the azimuthal angles of BS beam alignment. Here, a sectorized approximation to the beam pattern is assumed. If $\theta \in [\theta_0 - \frac{\Delta\omega}{2}, \theta_0 + \frac{\Delta\omega}{2}]$, where $\Delta\omega$ is the half power beamwidth, then the perfect

alignment of the transmitter beam is considered and its gain is denoted by G_{\max} . The gain, in case of a misaligned beam, is G_{\min} . The channel gain h follows Rayleigh or Rician distribution for LoS or NLoS links, respectively.

The signal-to-interference plus noise ratio (SINR) of the i^{th} user on the x^{th} subcarrier at the j^{th} BS is given by

$$\text{SINR}_i^j[x] = \frac{\mu_i^j[x]}{\sigma^2[x] + I_i^j[x]}, \quad (4.6)$$

where $I_i^j[x]$ represents the interference at the j^{th} BS for the i^{th} user on the x^{th} subcarrier.

The interference for the i^{th} user on subcarrier k_m at the m^{th} FAP operating on mmW band is given by

$$I_i^m[k_m] = \sum_{\substack{j=1 \\ j \neq m}}^M \sum_{f=1}^F \left(1 - \prod_{\substack{a=1 \\ a \neq m}}^{M_M} \mathbb{1}_{\rho_{f_j}^a[k_m]=0} \right) \mu_f^m[k_m] + \sum_{n=1}^N \left(1 - \prod_{\substack{j=1 \\ j \neq m}}^{M_M} \mathbb{1}_{\rho_n^j[k_m]=0} \right) \mu_n^m[k_m], \quad (4.7)$$

whereas the interference of the i^{th} user on subcarrier k at the m^{th} FAP operating on UHF band is given by

$$I_i^m[k] = \sum_{\substack{u=1 \\ u \neq i}}^I \left[\sum_{j=1}^M \left(1 - \prod_{a=1}^{M_U} \mathbb{1}_{\rho_{u_j}^a[k]=0} \right) \mu_u^m[k] + \prod_{j=1}^{M_M} \mathbb{1}_{\rho_u^j[k]=0} \mu_u^m[k] \right]. \quad (4.8)$$

where the indicator function $\mathbb{1}_{\{\rho\}} = 1$ if and only if $\rho = 0$.

The interference for the n^{th} MUE at MBS is given by

$$I_n^b[l] = \sum_{j=1}^M \sum_{i=1}^F \left(1 - \prod_{a=1}^{M_U} \mathbb{1}_{\rho_{ij}^a[k]=0} \right) \mu_{f_j}^b[l] + \sum_{\substack{i=1 \\ i \neq n}}^N \prod_{j=1}^{M_M} \mathbb{1}_{\rho_i^j[l]=0} \mu_n^b[l]. \quad (4.9)$$

The transmission power of all the users is limited to P^{\max} . Each link between the user and the BS causes individual circuit power. In macrocell, it is denoted by $P_{C(\text{MBS})}$ and it is represented as $P_{C(m)}$ in the m^{th} femtocell where $P_{C(\text{MBS})} = P_{C(m)} = P_C$. Thus, the total power is written as

$$P_T = \epsilon \sum_{j \in \mathcal{J}} \sum_{i \in \mathcal{I}} \sum_{x \in \mathcal{X}} \rho_i^j[x] p_i^j[x] + (N + FM) \times P_C, \quad (4.10)$$

where ϵ represents the inverse of power amplifier efficiency. The EE, in bits/sec/Watt, is the amount of energy required by the system to transmit data and is expressed as

$$\eta_{\text{EE}} = \max_{p_i^j} \frac{\sum_{j \in \mathcal{J}} \sum_{i \in \mathcal{I}} \sum_{x \in \mathcal{X}} R_i^j[x]}{\epsilon \sum_{j \in \mathcal{J}} \sum_{i \in \mathcal{I}} \sum_{x \in \mathcal{X}} \rho_i^j[x] p_i^j[x] + (N + FM) \times P_C}. \quad (4.11)$$

4.2 Problem Formulation

In our proposed scheme, two games are played in a hierarchical order. In the first game, each FAP decides between mmWave and UHF frequency bands with the goal to optimise its data rate forming a non-cooperative game. In the start, all FAPs have open access policy which allows them to connect with the MUEs to reduce the interference and maximise their rates. Let the fraction of the band allocated by the m^{th} FAP to the i^{th} user is de-

noted by $\omega_{i,m}$. This frequency band assignment to the FUEs and the MUEs by the FAPs forms the strategy space of FAPs in this game. Here, $\boldsymbol{\omega}_m = [\omega_{n_1,m_u}, \dots, \omega_{n_N,m_u}, \omega_{n_1,m_m}, \dots, \omega_{n_N,m_m}, \omega_{f_1,m_u}, \dots, \omega_{f_F,m_u}, \omega_{f_1,m_m}, \dots, \omega_{f_F,m_m}]^T$ is the strategy vector of m^{th} FAP where m_u represents the m^{th} FAP operating on UHF band and m_m represents the m^{th} FAP operating on mmWave band. $\boldsymbol{\omega}_{-m} = [\boldsymbol{\omega}_1^T, \dots, \boldsymbol{\omega}_{m-1}^T, \boldsymbol{\omega}_{m+1}^T, \dots, \boldsymbol{\omega}_M^T]^T$ shows the strategy vector of the other FAPs and $[\cdot]^T$ denotes the transpose operator. The utility function of the m^{th} FAP is the sum-rate of the FUEs and the MUEs connected to it.

$$\begin{aligned} \tilde{U}_m(\boldsymbol{\omega}_m, \boldsymbol{\omega}_{-m}) = & \sum_{i=1}^F \omega_{f_i,m} \log(1 + \text{SINR}_i^m) + \\ & \sum_{i=1}^N \omega_{n_i,m} \log(1 + \text{SINR}_i^m). \end{aligned} \quad (4.12)$$

The strategy space in this game for the m^{th} FAP is given as

$$\tilde{\chi}_m = \{\boldsymbol{\omega}_m \in [0, B]^N : \sum_{i=1}^{N_m \cup F_m} \omega_i^m = B\}. \quad (4.13)$$

The above constraint makes sure that frequency allocation is well defined by each FAP. The optimization problem for the m^{th} FAP, given the strategy vectors of other FAPs, is

$$\max_{\boldsymbol{\omega}_m \in \tilde{\chi}_m} (\boldsymbol{\omega}_m, \boldsymbol{\omega}_{-m}). \quad (4.14)$$

This non-cooperative game achieves convergence using the solution of PSNE.

A player achieves Nash equilibrium when

$$\tilde{U}_m(\boldsymbol{\omega}^*_m, \boldsymbol{\omega}^*_{-m}) \geq \tilde{U}_m(\boldsymbol{\omega}_m, \boldsymbol{\omega}^*_{-m}); \forall \boldsymbol{\omega}_m \in \tilde{\chi}_m, \quad (4.15)$$

where $\boldsymbol{\omega}_m$ represents the strategy vector of the m^{th} player and U_m represents the utility function.

The next game incorporates user association to maximise the sum-rate and EE of the network, where users evaluate their connectivity with the goal of maximizing their rates without affecting the network performance. The single-objective optimization problem becomes

$$\begin{aligned} & \max_{p_i^j} \quad \eta_{\text{EE}} \\ \text{s.t.} \quad & \sum_{j \in \mathbb{J}} R_i^j[\boldsymbol{\omega}] \geq R_{\min}, \quad \forall i, \\ & \sum_{j \in \mathbb{J}} p_i^j[\boldsymbol{\omega}] \leq P_i^{\max}, \quad \forall i, \\ & \sum_{\substack{j \in \mathbb{J} \\ j \neq m}} \sum_{i \in \mathbb{I}} g_{ij}[\boldsymbol{\omega}] p_i^j[\boldsymbol{\omega}] \leq I[\boldsymbol{\omega}], \quad \forall \boldsymbol{\omega}, \end{aligned} \quad (4.16)$$

where first constraint ensures the achieved rate of the user is at least as high as R_{\min} . Second and third constraints limit the maximum transmit power of the users to maximise EE. Here, we have replaced the subcarriers with the fraction of band, $(\omega_{i,j})$, allocated to the i^{th} user by the j^{th} BS. Let the index set of frequency band allocated to users be $\mathbb{W} = \{\omega_1, \omega_2, \dots, \omega_I\}$.

The objective function can then be expressed as

$$U(\eta_{EE}) = \max_{p_i^j} \left[\sum_{j \in \mathcal{J}} \sum_{i \in \mathcal{I}} \sum_{\omega \in \mathcal{W}} R_i^j[\omega] - \eta_{EE} \left(\epsilon \sum_{j \in \mathcal{J}} \sum_{i \in \mathcal{I}} \sum_{\omega \in \mathcal{W}} p_i^j[\omega] + (N + FM) \times P_C \right) \right]. \quad (4.17)$$

The Lagrangian function of the above equation becomes

$$\begin{aligned} L(p, \boldsymbol{\lambda}, \boldsymbol{\mu}, \boldsymbol{\nu}) = & \sum_{m \in \mathcal{J}} \sum_{i \in \mathcal{I}} \sum_{\omega \in \mathcal{W}} R_i^j[\omega] - \eta_{EE} \left(\epsilon \sum_{j \in \mathcal{J}} \sum_{i \in \mathcal{I}} \sum_{\omega \in \mathcal{W}} p_i^j[\omega] \right. \\ & \left. + (N + FM) \times P_C \right) + \sum_{i \in \mathcal{I}} \lambda_i \left(\sum_{j \in \mathcal{J}} \sum_{\omega \in \mathcal{W}} R_i^j[\omega] - R_{\min} \right) + \sum_{i \in \mathcal{I}} \mu_i \\ & \left(P_i^{\max} - \sum_{j \in \mathcal{J}} \sum_{\omega \in \mathcal{W}} p_i^j[\omega] \right) + \sum_{\omega \in \mathcal{W}} \nu_{\omega} \left(I[\omega] - \sum_{j \in \mathcal{J}} \sum_{i \in \mathcal{I}} p_i^j[\omega] g_{ij}[\omega] \right), \end{aligned} \quad (4.18)$$

where $\boldsymbol{\lambda} = \{\lambda_1, \lambda_2, \dots, \lambda_I\}$, $\boldsymbol{\mu} = \{\mu_1, \mu_2, \dots, \mu_I\}$ and $\boldsymbol{\nu} = \{\nu_{\omega_1}, \nu_{\omega_2}, \dots, \nu_{\omega_I}\}$ are the Lagrange multiplier vectors associated with R_{\min} , optimal transmit power and cross-tier interference threshold constraints, respectively.

The Lagrangian dual function is

$$g(\boldsymbol{\lambda}, \boldsymbol{\mu}, \boldsymbol{\nu}) = \max_{p_i^j} L(p_i^j, \boldsymbol{\lambda}, \boldsymbol{\mu}, \boldsymbol{\nu}). \quad (4.19)$$

$$\begin{aligned} g(\boldsymbol{\lambda}, \boldsymbol{\mu}, \boldsymbol{\nu}) = & \sum_{\omega \in \mathcal{W}} g_{\omega}(\boldsymbol{\lambda}, \boldsymbol{\mu}, \boldsymbol{\nu}) - \epsilon \eta (N + FM) P_C + \\ & \sum_{\omega \in \mathcal{B}} \nu_{\omega} I[\omega] + \sum_{i \in \mathcal{I}} \mu_i P_i^{\max} - \sum_{i \in \mathcal{I}} \lambda_i R_{\min}, \end{aligned} \quad (4.20)$$

where $g_\omega(\boldsymbol{\lambda}, \boldsymbol{\mu}, \boldsymbol{\nu})$ is defined as

$$g_\omega(\boldsymbol{\lambda}, \boldsymbol{\mu}, \boldsymbol{\nu}) = \max_{p_i^j} \left[\sum_{j \in \mathcal{J}} \sum_{i \in \mathcal{I}} R_i^j[\omega] - \eta \epsilon \sum_{j \in \mathcal{J}} \sum_{i \in \mathcal{I}} p_i^j[\omega] + \sum_{i \in \mathcal{I}} \sum_{j \in \mathcal{J}} \lambda_i R_i^j[\omega] - \sum_{i \in \mathcal{I}} \sum_{j \in \mathcal{J}} \mu_i p_i^j[\omega] - \sum_{i \in \mathcal{I}} \sum_{j \in \mathcal{J}} \nu_w p_i^j[\omega] g_{ij}[\omega] \right]. \quad (4.21)$$

$$g_\omega(\boldsymbol{\lambda}, \boldsymbol{\mu}, \boldsymbol{\nu}) = \max_{p_i^j} \left(\sum_{j \in \mathcal{J}} \sum_{i \in \mathcal{I}} B_w \log(1 + \beta_i^j p_i^j[\omega]) [1 + \lambda_i] - \sum_{j \in \mathcal{J}} \sum_{i \in \mathcal{I}} (\mu_i + \epsilon \eta_{EE} + \nu_w g_{ij}[\omega]) p_i^j[\omega] \right). \quad (4.22)$$

where β_i^j represents channel-to-interference and noise ratio of the i^{th} user connected to j^{th} BS.

We have decomposed the above dual problem into a hierarchical framework of two sub-problems. The master sub-problem uses sub-gradient method to update the Lagrangian multipliers whereas the slave sub-problem consisting of K sub-problems solved in parallel is responsible for computing power for given values of η_{EE} and Lagrange multipliers. The first derivative of (4.22) w.r.t $p_i^j[\omega]$ is

$$\frac{\partial g_\omega(\boldsymbol{\lambda}, \boldsymbol{\mu}, \boldsymbol{\nu})}{\partial p_i^j[\omega]} = \frac{B_w [1 + \lambda_i] \beta_i^j p_i^j[\omega]}{\ln 2 (1 + \beta_i^j p_i^j[\omega])}. \quad (4.23)$$

Now, by applying KKT conditions, we get

$$\left. \frac{\partial g_\omega(\boldsymbol{\lambda}, \boldsymbol{\mu}, \boldsymbol{\nu})}{\partial p_i^j[\omega]} \right|_{p_i^j[\omega] = p_i^j[\omega]^*} = 0 \quad (4.24)$$

Hence,

$$p_i^j[\omega] = \begin{cases} \left(\frac{B_w [1+\lambda_i]}{\ln 2 (\mu_i + \epsilon \eta_{EE} + \nu_w g_{ij}[\omega])} - \frac{1}{\beta_i^j} \right)^+ & \omega > 0, \\ 0 & \text{otherwise.} \end{cases}$$

The optimal solution of (4.17) can be expressed as

$$p_i^{j*} = \min(p_i^j[\omega], P_i^{\max}) \quad (4.25)$$

Now, we can update the Lagrange multipliers as

$$\lambda_i(k+1) = \left(\lambda_i(k) - \frac{\alpha^1}{\sqrt{k}} \left(\sum_{j \in \mathcal{J}} \sum_{\omega \in \mathcal{W}} R_i^j[\omega] - R_{\min} \right) \right)^+, \quad (4.26)$$

$$\mu_i(k+1) = \left(\mu_i(k) - \frac{\alpha^2}{\sqrt{k}} \left(P_i^{\max} - \sum_{j \in \mathcal{J}} \sum_{\omega \in \mathcal{W}} p_i^j[\omega] \right) \right)^+, \quad (4.27)$$

$$\nu_w(k+1) = \left(\nu_w(k) - \frac{\alpha^3}{\sqrt{k}} \left(I[\omega] - \sum_{i \in \mathcal{I}} \sum_{j \in \mathcal{J}} p_i^j[\omega] g_{ij}[\omega] \right) \right)^+. \quad (4.28)$$

where α is the step length and i is the iteration number. These equations continues to update until convergence is achieved.

4.3 Simulation Results

We consider a two-tier HetNet with a single macrocell of radius 500 m where femtocells with the radius of 50 m each are uniformly overlaid on it. The users are also uniformly scattered over the area. The bandwidth, B_1 , for mmWave band is 2 GHz and for UHF band the bandwidth, B_2 , is 20 MHz [22]. The maximum transmit power P_{\max} is set to be 0.4 W and the minimum

acceptable data rate for the MUEs, R_{\min} , is 0.25 Mbps. These thresholds are same for all users. The value of P_C is fixed to be 0.1 W, ϵ is 38% and the interference threshold is 1.1943×10^{-14} W unless stated otherwise. The parameters for path loss models are listed in Table. 5.2.

We have analysed the sum-rate and EE of the proposed hybrid HetNet and all-UHF HetNet with and without power control mechanism. This proposed scheme allows FAPs to decide their access policy in the best interest of their users and MUEs to finalize their connectivity to maximise the EE while fulfilling all the constraints. It outperforms the all-UHF scheme as shown in Fig. 4.2 and Fig. 4.3 because the UHF network shows better coverage probabilities at lower SINR thresholds as they provide higher SINR at the BS for the cell edge users. The mmWave network, on the other hand, provides better coverage when users are located near the BS as it undergoes lower interference from the neighbouring users. Thus, a fusion of both networks leads to better performance. The increasing trend in all schemes in the sum-rate and EE with increasing number of FAPs is due to the fact that as FAPs increases, they connect more MUEs and thus reduce the interference in the network. The performance of this hybrid scheme further improves when power control is applied. By limiting transmit power to an optimal value, the cross-tier interference reduces, which increases the SINR; thus improving sum-rate and EE.

Fig. 4.4 reveals that the EE of a hybrid HetNet increases as the value of interference threshold decreases. The trend shows that as the threshold level decreases, the corresponding transmit power of the users decreases, which reduces the interference. This reduction in the interference leads to

Table 4.1: Simulation Parameters.

Parameter	Value	Parameter	Value
$f_c(\text{mmW})$	73 GHz	$f_c(\text{UHF})$	2.4 GHz
α_L	2.2	α_N	3.3
σ_{Ω_L}	5.2 dB	σ_{Ω_N}	7.38 dB
σ_{Ψ}	4 dB	K-factor (Rician)	4 dB

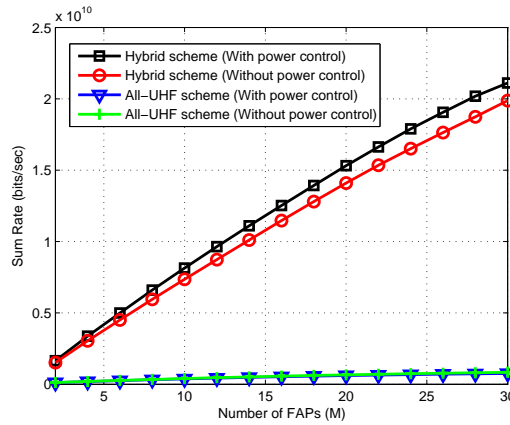


Figure 4.2: Sum-rate of a hybrid HetNet and all-UHF HetNet with and without power control with varying number of FAPs for $N=100$ and $F=5$.

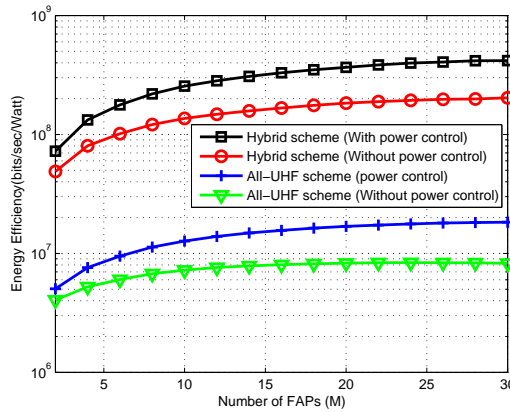


Figure 4.3: Energy Efficiency of a hybrid HetNet and all-UHF HetNet with and without power control with varying number of FAPs for $N=100$ and $F=5$.

the increment in the SINR; thus improving sum-rate and EE.

Fig. 4.5 shows that the trend of EE associated with the density of mmWave FAPs. We can observe that the EE is very low when the density of mmWave FAPs is zero i.e. all UHF scheme. As the density of FAPs operating on mmWave increases, the users located near the FAPs will get better coverage and thus data rates and EE increases. This trend becomes steady after a while as the FAPs serving the MUEs start dominating. This is due of the fact that the mmWave FAPs restrict their ability to form links over long distances due to greater path loss associated with mmWave and it is in the best interest of the network that these FAPs should operate on UHF band. Thus, a hybrid approach offers better data rates and EE than all-UHF and all-mmWave femto-tier network. From the figure, we can also observe that as the radius of the network increases, the distance between the MUEs and the FAPs increases, which will reduce the interference. Thus relatively less MUEs connect with the FAPs and the near located users play the major role making more FAPs to operate on mmWave due to better coverage. This trend follows up to a certain radius of the network, then it starts decreasing if we further increase the radius as the SINR start decreasing.

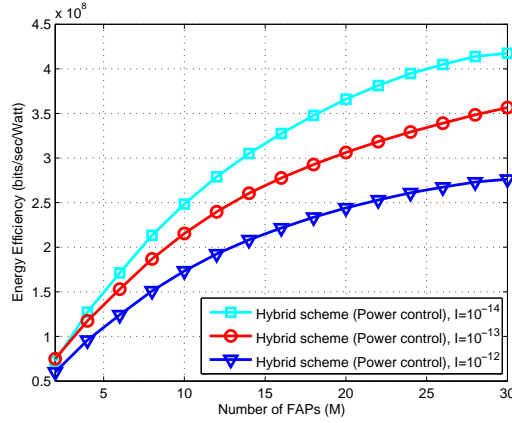


Figure 4.4: Energy Efficiency of a hybrid HetNet with power control for various interference threshold with varying number of FAPs for $N=100$ and $F=5$.

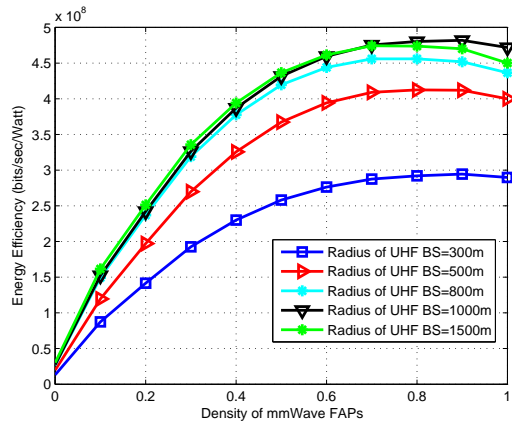


Figure 4.5: Energy Efficiency of a hybrid HetNet with power control with varying density of mmWave FAPs for $M=15$, $F=5$ and $N=100$.

Chapter 5

5G HetNets Exploiting

Multi-Slope Path Loss Model

In this chapter, we extend the dual slope analysis on the downlink of a Het-Net with picocells overlaid on a macrocell. The user association is done to offload the traffic to pico-tier using dual slope path loss model. We have considered different slopes before and beyond the critical distance, which can be used to approximate the two regimes of LOS and NLOS links. This distance is environment dependent, which increases with less blocking environment, but can be approximated by taking the average LOS link distance. The performance enhancement with dual slope model is significant in achieving better offloading compared to single slope model in HetNets. The user association and load balancing is analyzed and we show that the biasing with dual slope path loss model outperforms the conventional biasing schemes. The dual slope path loss model leads to steering of users to the nearby small cells, thus offloading the traffic from macro-tier.

5.1 System Model

Consider the downlink of a two-tier HetNet composed of $M - 1$ picocell base station (PBSs) overlaid on a macrocell. A snapshot of a two-tier HetNet is shown in Fig. 5.1 where both tiers use dual-slope path loss model. The path loss models are explained in detail in Section 5.1.1. The macrocell base station (MBS) is represented by m_o whereas the set of all the base stations (BSs) in the system is given as $\mathbb{M} = \{m_o, m_1, \dots, m_{M-1}\}$. Let $\mathbb{N} = \mathbb{N}_M \cup \mathbb{N}_o$ be the set of all users deployed randomly over the entire area. The set of macrocell user equipments (MUEs) is denoted by \mathbb{N}_o and the set of picocell users equipments (PUEs) is represented by $\mathbb{N}_M = \bigcup_{m=1}^{M-1} \mathbb{N}_m$ where \mathbb{N}_m is the set of PUEs served by the m^{th} PBS.

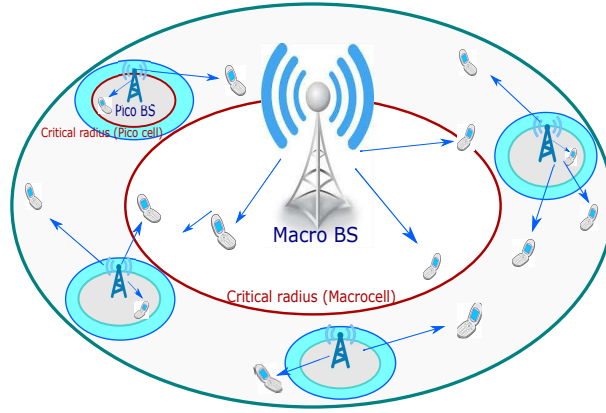


Figure 5.1: A two-tier heterogeneous network with red circles showing the critical radius of picocell and macrocell.

5.1.1 Path Loss Models

In this section, we present different path loss models to model the large scale fading in the network. The single slope path loss model is given as

$$L(d)[\text{dB}] = 20 \log_{10}\left(\frac{4\pi}{\lambda_c}\right) + 10\alpha \log_{10}(d) + \xi, \quad (5.1)$$

where λ_c corresponds to the carrier wavelength, α is the path loss exponent and ξ is a Gaussian random variable (RV) with zero mean and σ^2 variance.

The single slope path loss model is the standard model, which falls short in accurately capturing the path loss exponent dependence on the physical environment in dense and millimeter wave capable networks. These limitations lead to the consideration of dual-slope path loss model in future networks.

The dual-slope path loss model is given as

$$L(d)[\text{dB}] = \begin{cases} \beta + 10\alpha_1 \log_{10}(d) + \xi & d \leq r_c \\ \beta + 10\alpha_1 \log_{10}(r_c) \\ + 10\alpha_2 \log\left(\frac{d}{r_c}\right) + \xi & d > r_c \end{cases}, \quad (5.2)$$

where d is the distance in meters and r_c is the critical distance. β represents the floating intercept, α_1 and α_2 are the slopes for below and beyond critical radius, r_c .

This dual slope model can be generalized into N-slope model as

$$L(d)[\text{dB}] = \begin{cases} l_1(d) = \beta + 10\alpha_1 \log_{10}(d) + \xi & 0 < d \leq r_c^{(1)} \\ l_2(r_c^{(1)}, d) = l_1(r_c^{(1)}) + \\ 10\alpha_2 \log\left(\frac{d}{r_c^{(1)}}\right) & r_c^{(1)} < d \leq r_c^{(2)} \\ l_3(r_c^{(1)}, r_c^{(2)}, d) = l_2(r_c^{(1)}, r_c^{(2)}) \\ + 10\alpha_3 \log\left(\frac{d}{r_c^{(2)}}\right) & r_c^{(2)} < d \leq r_c^{(3)} \\ \cdot & \cdot \\ \cdot & \cdot \\ \cdot & \cdot \\ l_N(r_c^{(1)}, r_c^{(2)}, \dots, r_c^{(N-1)}, d) = \\ l_{N-1}(r_c^{(1)}, r_c^{(2)}, \dots, r_c^{(N-1)}) + \\ 10\alpha_N \log\left(\frac{d}{r_c^{(N-1)}}\right) & d > r_c^{(N-1)} \end{cases}, \quad (5.3)$$

where α_n , $n = \{1, \dots, N\}$, is the path loss exponent such that $0 \leq \alpha_1 \leq \alpha_2 \leq \dots \leq \alpha_N$. The critical distance is denoted as $r_c^{(n)}$, $n = \{1, \dots, N-1\}$, such that $r_c^{(1)} \leq r_c^{(2)} \leq \dots \leq r_c^{(N)}$.

5.1.2 User Association

This paper considers different approaches for user association. We assume open access, which allows users to connect to any tier. We analyze the cell association based on minimum path loss, maximum biased received power and maximum biased rate.

Table 5.1: Parameter Notation.

Parameter	Symbols
Set of Tiers	\mathbb{I}
Set of BSs	\mathbb{M}
Set of Users	\mathbb{N}
Transmit Power	$p_{n,m}$
Channel Gain	$h_{n,m}$
Channel-to-interference-plus-noise Ratio	$\gamma_{n,m}$
i^{th} tier Biasing Factor	θ_i
Critical Radius	r_c
Path Loss Exponent (Single-Slope Model)	α
Path Loss Exponents (Dual-Slope Model)	$[\alpha_1, \alpha_2]$
Floating intercept (Dual Slope)	β
m^{th} BS Power Budget	P_m^{\max}
Noise Power	N_0

Minimum Path Loss

We first consider the association on the basis of path loss, where users are associated with the BS which gives the lowest path loss. The n^{th} user is associated with the m^{th} BS that maximizes

$$\arg \max_m \frac{1}{L(d_{n,m})}, \quad (5.4)$$

where $d_{n,m}$ is the distance between the n^{th} user and the m^{th} BS.

Maximum Biased Received Power

The association is determined on the basis of received power, where users are associated with the BS that serves the maximum biased received power. The n^{th} user is associated with the m^{th} BS that maximizes

$$\arg \max_m \frac{\theta_i P_m^{\max}}{L(d_{n,m})}, \quad (5.5)$$

where P_m^{\max} is the maximum transmit power of the m^{th} BS and θ_i is the bias factor for the i^{th} tier and all the BSs in the particular tier use the identical bias value. This case can be reduced to maximum received power association by putting $\theta_i = 1$. This paper assumes the bias value for macro-tier, $\theta_1 = 0$ dB and it varies between 0 dB to 30 dB for pico-tier, in case of biased received power association.

Maximum Biased Rate

The user association is decided on the basis of achievable rate. The n^{th} user is associated with the m^{th} BS that gives the maximum biased rate, i.e,

$$\arg \max_m \theta_i R_{n,m}, \quad (5.6)$$

where θ_i is the bias factor for the i^{th} tier. This paper assumes the bias value for macro-tier, $\theta_1 = 1$, in case of biased rate association. The achievable rate, $R_{n,m}$, in (b/s/Hz) can be formally defined as

$$R_{n,m} = \log_2(1 + p_{n,m}\gamma_{n,m}), \quad (5.7)$$

where $p_{n,m}$ is the transmit power from the m^{th} BS to the n^{th} user. $\gamma_{n,m}$ is the channel-to-noise ratio between the m^{th} BS and the n^{th} user.

The channel-to-noise ratio is defined as

$$\gamma_{n,m} = \frac{|h_{n,m}|^2}{N_0}, \quad (5.8)$$

where N_0 represents the noise power and $h_{n,m}$ corresponds to the channel gain. In this paper, we assume that each user is associated with one BS at a time.

5.2 Simulation Results

We consider a two-tier HetNet with a single macrocell of radius 500 m where picocells are uniformly overlaid on the edge of it. The maximum transmit

Table 5.2: Simulation Parameters.

Parameter	Value	Parameter	Value
β	42.1 dB	σ_ξ	6.9 dB
α	3	f_c	2.4 GHz
$r_m(\text{macrocell})$	350 m	$r_m(\text{picocell})$	50 m

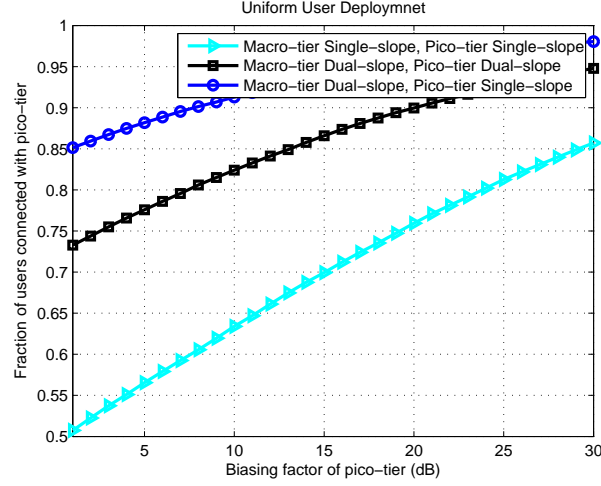


Figure 5.2: Fraction of users connected to pico-tier when biased received power association is used across varying biasing factor of pico-tier, θ_2 , for $N = 100$, $M = 4$, $\theta_1 = 0$ dB, $[\alpha_1, \alpha_2](\text{Macro-tier}) = [4, 5]$ and $[\alpha_1, \alpha_2](\text{Pico-tier}) = [3, 4]$.

power of MBS and PBS, P_m^{\max} , is set to 46 dBm and 30 dBm, respectively. The power spectral density of noise is -174 dBm/Hz. The parameters used for path loss models are listed in Table 5.2 [50], unless stated otherwise.

For user deployment, two different schemes are considered. In the first scheme, users are uniformly scattered over the entire area whereas, in the second scheme, high user density exists outside the critical radius of the macrocell.

Fig. 5.2 and Fig. 5.3 show the fraction of users associated with pico-tier for maximum biased received power association and uniform user deploy-

ment. The values of path loss exponents used in these figures represent harsh and moderate environment conditions, respectively.

In Fig. 5.2, biasing effect is investigated by varying the bias factor of the pico-tier with no biasing of the macro-tier for harsh environment conditions. An increasing trend in user offloading can be observed with the increasing pico-tier bias factor as biasing improves the received signal strength originating from PBSs. The figure reveals that biasing with both single and dual slope models is beneficial for offloading. However, with dual-slope model, this effect is stronger as dual slope model better approximates the links. This figure also compares the offloading performance of the network while exploiting single-slope and dual-slope path loss models. The figure shows that the offloading is maximum with dual slope model in the macrocell, as higher path loss exponents of the macro-tier directs the users to the nearby BSs due to highly attenuated long distance links between users and MBS. As the user leaves the critical radius of the macrocell, the NLoS path loss exponent increases, which further decreases the signal strength and users are offloaded to pico-tier. In harsh environment conditions, applying dual slope model in the macrocell offloads the traffic to pico-tier and if dual slope model is applied on picocells too, it prevents the offloading up to some extent as NLoS exponent of pico-tier is greater than the PLE used for single slope model.

Fig. 5.3 shows the fraction of users associated with pico-tier for moderate environment conditions and rest of the assumptions are same as used in Fig. 5.2. This figure reveals that the performance of the scheme with dual slope model in both tiers is better than the scheme where dual slope model is

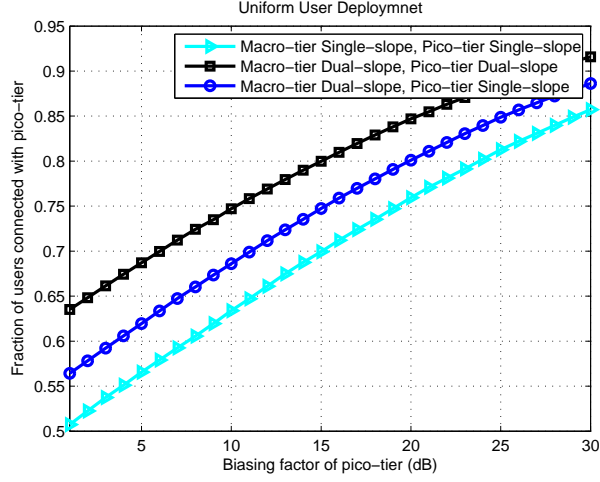


Figure 5.3: Fraction of users connected to pico-tier when biased received power association is used across varying biasing factor of pico-tier, θ_2 , for $N = 100$, $M = 4$, $\theta_1 = 0$ dB, $[\alpha_1, \alpha_2](\text{Macro-tier}) = [3, 4]$ and $[\alpha_1, \alpha_2](\text{Pico-tier}) = [2, 4]$.

applied on macro-tier only, unlike the previous case. This is because of the fact that in moderate environment conditions, lower path loss exponent within the critical radius induces less attenuation. The offloading to pico-tier is comparatively less when dual slope model is used in macro-tier only as some users residing within the critical radius of the macrocell might prefer MBS over PBSs because smaller PLE is used within the critical radius of the macrocell, resulting in reduced attenuation. The offloading improves when dual slope model is applied on pico-tier too, as more users are pushed toward nearby PBSs with less attenuated coverage region.

Fig. 5.4 shows the fraction of users associated with pico-tier across varying biasing factor of pico-tier. Maximum received power association and high edge user density is considered with moderate environment conditions. The figure shows that the offloading is relatively high in this case as compared

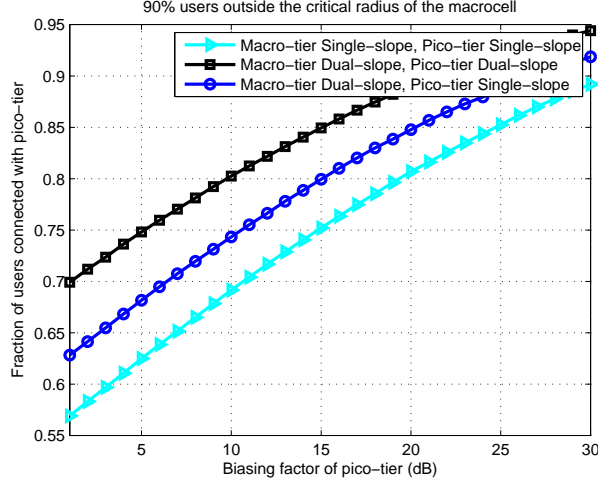


Figure 5.4: Fraction of users connected to pico-tier when biased received power association is used across varying biasing factor of pico-tier, θ_2 , for $N = 100$, $M = 4$, $\theta_1 = 0$ dB, $[\alpha_1, \alpha_2](\text{Macro-tier}) = [3, 4]$ and $[\alpha_1, \alpha_2](\text{Pico-tier}) = [2, 4]$.

to the previous case where uniform user deployment is used as shown in fig. 5.3. This is due to the fact that the picocells are deployed on the edge of the macrocell where the density of users is high for this case and thus, the offloading improves. This figure further reveals that the dual slope model needs less biasing to achieve a particular offloading as compared to single slope model.

In Fig. 5.5, the path loss association is considered to show the impact of BS density on the user offloading to pico-tier. The figure shows that as the density of PBSs increases, the distances of the users from the PBSs decreases, which in turn decreases the path losses and the load is shifted to the less congested PBSs. The trend is sharp in the start as the edge users start connecting to the pico-tier, which is more rapid in case of dual slope model. This offloading almost becomes invariant with further increase in the

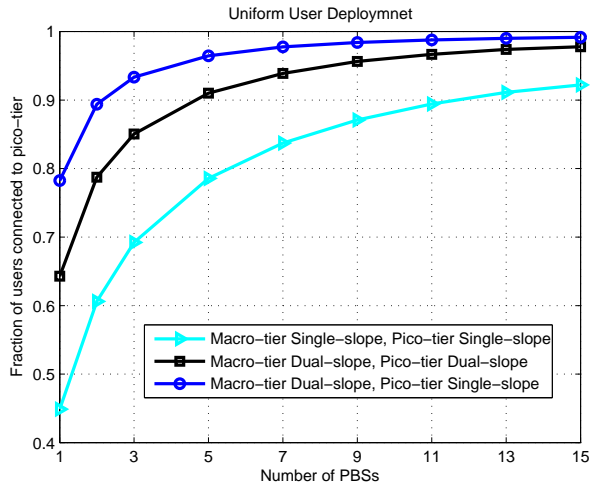


Figure 5.5: Fraction of users connected to pico-tier when path loss association is used across varying density of PBSs for $N = 100$, $\theta_1 = \theta_2 = 0$ dB, $[\alpha_1, \alpha_2](\text{Macro-tier}) = [4, 5]$ and $[\alpha_1, \alpha_2](\text{Pico-tier}) = [3, 4]$.

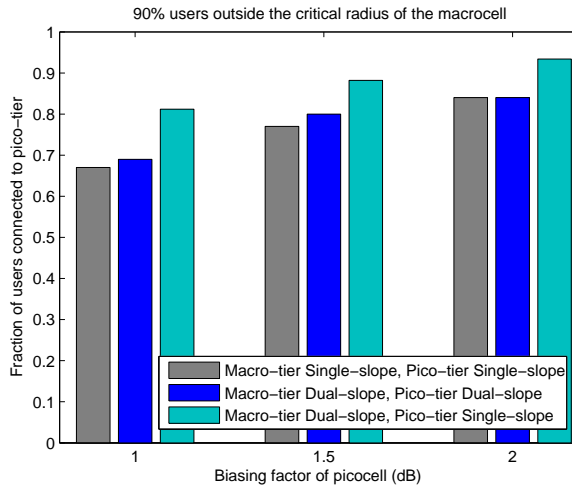


Figure 5.6: Fraction of users connected to pico-tier when association is done based on biased maximum rate across varying pico-tier bias factor, θ_2 , for $N = 50$, $M = 4$, $\theta_1 = 0$ dB, $[\alpha_1, \alpha_2](\text{Macro-tier}) = [4, 5]$ and $[\alpha_1, \alpha_2](\text{Pico-tier}) = [3, 4]$.

PBSs density in case of dual slope model.

Fig. 5.6 shows the user association in case of rate maximization for high

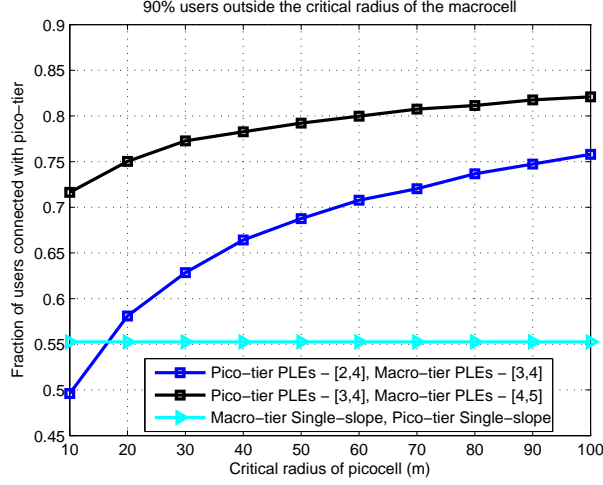


Figure 5.7: Fraction of users connected to pico-tier when biased received power association is used across varying critical radius of picocell for $N = 100$, $M = 4$, $\theta_1 = \theta_2 = 0$ dB

edge user density. Similar trend as in Fig. 5.2 can be seen here. The fraction of the users associated to pico-tier increases with the dual slope model but the improvement in offloading, is comparatively less when compared to other two association schemes. This is because of the fact that the dual slope model is more beneficial for median users as compared to the edge users in terms of high data rates. Thus, less number of users offload to pico-tier in order to maximize their rate, however, the offloading is better as compared to the single slope model. This figure also reveals that the increase in the bias factor for pico-tier improves the offloading, as users get better biased rate from the pico-tier.

In fig. 5.7, we demonstrate the impact of critical radius of the picocell on the performance of the network for high edge user deployment. As the critical radius of the picocell increases, more users start entering within r_c , the attenuation decreases due to smaller PLE and the users residing within

r_c prefer PBSs due to less attenuated links. However, the increasing trend in the sum rate is sharp in the beginning and then it starts slowing down with further increase in r_c . This is because of the fact that as r_c increases, the user offloading to pico-tier increases but the distance between the PBSs and the users also increases and the approximation of LoS links within the critical radius of picocells start affecting. The figure further reveals the impact of path loss exponents of the dual slope model on user offloading. It can be seen from the figure that the case with larger path loss exponents shows better offloading as they induce higher attenuation in the cell and users prefer nearby BSs. The user offloading in case of single slope model is minimum as it does not accurately characterize the network, which cause performance degradation.

Chapter 6

Conclusions

In this thesis, we discussed and analyzed various promising technologies for 5G wireless communication systems. This work proposed QoS aware resource optimization to maximize data rates and EE in HetNets integrated with mmWave technology, user-centricity and dual slope path loss model. This thesis can be concluded in three parts

- Firstly a game-theoretic framework for resource allocation is formulated in chapter 3, which allows the FAPs to strategically decide between the conflicting access modes while optimizing their allocated resources. It also enables the MUEs to decide their connectivity while acquiring their stable action profiles. The main focus of the players is to optimize the tradeoff between reducing interference and the cost of allocated resources. This hierarchical game framework optimizes the data rates of the FUEs and the MUEs while achieving the Nash equilibrium. We have applied low complexity user-centric distributed approach to improve the performance of the network and the simulation results

have proved that the proposed algorithm significantly outperforms the network-centric scheme.

- Secondly, a hierarchical framework to optimise EE in a two-tier hybrid HetNet is proposed, in chapter 4, while incorporating maximum transmit power and interference constraint. This scheme allows FAPs to decide their access policy along with the selection of frequency band in between sub-6 GHz and mmWave. The user association method is then carried out to maximise the EE. The proposed game framework is solved using PSNE for outer layer and dual decomposition approach for inner layer. Simulation results show that in contrast to the all-UHF network, hybrid networks promise performance enhancement in terms of EE. The performance of the proposed design can be further improved using power control mechanism that aims at limiting the interference and increasing the SINR.
- Lastly, in chapter 5, we analyzed the impact of dual slope path loss model on the performance of a downlink multi-tier HetNet where different path loss exponents are used for different ranges. The user association is done to offload the traffic from macro-tier to pico-tier under single and dual slope path loss models. Simulation results suggest that the dual slope model shows significant improvement in terms of load balancing in comparison to single slope model, which does not measure the path loss exponent dependence on the link distance accurately. With the dual slope model, more users offload to pico-tier with lower biasing as compared to single slope model. We also observed the effect

of path loss exponents of dual slope model on the user association in multi-tier network. The above results strengthen the position of multi slope path loss model as a potential substitute for standard path loss model in the ever denser future networks.

Bibliography

- [1] Q. Ye, B. Rong, Y. Chen, M. Al-Shalash, C. Caramanis, and J. G. Andrews, “User association for load balancing in heterogeneous cellular networks,” *IEEE Trans. on Wireless Commun.*, vol. 12, no. 6, pp. 2706–2716, 2013
- [2] H. Munir, S. A. Hassan, H. Parveiz, Q. Ni, “A game theoretical network-assisted user-centric design for resource allocation in 5G heterogeneous networks”, *IEEE Vehicular Tech. Conf. (VTC-Spring)*, May, 2016.
- [3] Hu, R. Q., Qian, Y., Kota, S., Giambene, G., “HetNets - A New Paradigm for Increasing Cellular Capacity and Coverage [Guest Editorial]” - *IEEE Wireless Communications*, vol. 18, no. 3, pp. 8–9, June 2011.
- [4] A. Damnjanovic, J. Montojo, Y. Wei, T. Ji, T. Luo, M. Vajapeyam, T. Yoo, O. Song, and D. Malladi, “A survey on 3GPP heterogeneous networks,” *IEEE Wireless Communications*, vol. 18, no. 3, pp. 10–21, 2011.
- [5] A. Ghosh, N. Mangalvedhe, R. Ratasuk, B. Mondal, M. Cudak, E. Visotsky, T. A. Thomas, J. G. Andrews, P. Xia, H. S. Joet al., “Heteroge-

- neous cellular networks: From theory to practice,” *IEEE Communications Magazine*, vol. 50, no. 6, pp. 54–64, 2012.
- [6] D. Lopez-Perez, I. Guvenc, G. De la Roche, M. Kountouris, T. Q. Quek, and J. Zhang, “Enhanced intercell interference coordination challenges in heterogeneous networks,” *IEEE Wireless Commun.*, vol. 18, no. 3, pp. 22–30, 2011.
- [7] S. W. Hasan and S. A. Hassan, “Fuzzy Logic-based Downlink Subchannel Allocation for Capacity Maximization in OFDMA Femtocells”, IEEE International Wireless Communications and Mobile Computing Conference (IWCMC), Aug, 2015, Croatia.
- [8] R. Zahid and S. A. Hassan, “Stochastic Geometry-based Analysis of Multiple Region Reverse Frequency Allocation Scheme in Downlink Het-Nets”, IEEE International Wireless Communications and Mobile Computing Conference (IWCMC), Aug, 2015, Croatia.
- [9] R. Hu and Y. Qian, “An energy efficient and spectrum efficient wireless heterogeneous network framework for 5G systems”, *IEEE Commun. Mag.*, vol. 52, no. 5, pp. 94–101, 2014.
- [10] H. Pervaiz, L. Musavian, and Q. Ni, “Energy and spectrum efficiency trade-off for Green Small Cell Networks,” *IEEE International Conf. on Commun. (ICC)*, pp. 5410-5415, 2015.
- [11] J. Liu, D. Wang, J. Wang, J. Li, J. Pang, G. Shen, Q. Jiang, H. Sun, and Y. Meng, “Uplink power control and interference coordination for

- heterogeneous network,” *IEEE International Symposium on Personal Indoor and Mobile Radio Communications (PIMRC)*, pp. 519–523, 2012.
- [12] V. Chandrasekhar, J. G. Andrews, and A. Gatherer, “Femtocell networks: a survey,” *IEEE Commun. Mag.*, vol. 46, no. 9, pp. 59–67, 2008
- [13] P. Xia, V. Chandrasekhar, and J. G. Andrews, “Open vs. closed access femtocells in the uplink,” *IEEE Trans. Wireless Commun.*, vol. 9, no. 12, pp. 3798–3809, 2010.
- [14] D. L’opez-P’erez, A. Valcarce, G. De La Roche, and J. Zhang, “OFDMA femtocells: A roadmap on interference avoidance,” *IEEE Commun. Mag.*, vol. 47, no. 9, pp. 41–48, 2009.
- [15] D. Choi, P. Monajemi, S. Kang, and J. Villasenor, “Dealing with loud neighbors: The benefits and tradeoffs of adaptive femtocell access,” *Proc IEEE Global Telecommun. Conf. (GLOBECOM)*, pp. 1–5, Dec. 2008.
- [16] H.-S. Jo, P. Xia, and J. G. Andrews, “Open, closed, and shared access femtocells in the downlink,” *EURASIP Journal on Wireless Commun. and Networking*, vol. 2012, no. 1, pp. 1–16, 2012.
- [17] X. Kang, R. Zhang, and M. Motani, “Price-based resource allocation for spectrum-sharing femtocell networks: A stackelberg game approach,” *IEEE Journal on Selected Areas in Communications*, vol. 30, no. 3, pp. 538–549, 2012.
- [18] T. S. Rappaport, R. W. Heath Jr., R. C. Daniels, J. N. Murdock, *Milimeter Wave Wireless Communication*, Prentice Hall, 2014.

- [19] S.Q. Xiao, M.T. Zhou and Y.Zhang, “Millimeter wave technology in wireless PAN, LAN, and MAN.” *CRC Press*, 2008.
- [20] Z. Gao, L. Dai, D. Mi, Z. Wang, M. A. Imran, and M. Z. Shakir, “Mmwave massive-mimo-based wireless backhaul for the 5G ultra-dense network,” *IEEE Wireless Commun.*, vol. 22, no. 5, pp. 13–21, 2015.
- [21] A. Ghosh, T. A. Thomas, M. C. Cudak, R. Ratasuk, P. Moorut, F. W. Vook, T. S. Rappaport, G. R. MacCartney, S. Sun, S. Nie, “Millimeter wave enhanced local area systems: A high data rate approach for future wireless networks,” *IEEE J. Sel. Areas Commun.*, vol. 32, no. 6, pp.1152–1163, Jun. 2014.
- [22] S. Singh, M. N. Kulkarni, A. Ghosh, and J. G. Andrews, “Tractable model for rate in self-backhauled millimeter wave cellular networks”, *IEEE J. Sel. Areas Commun.*, vol. 33, no. 10, pp. 2196–2211, 2015.
- [23] S. Rangan, T. S. Rappaport, and E. Erkip, “Millimeter-wave cellular wireless networks: Potentials and challenges”, *IEEE Proceedings*, vol. 102, no. 3, pp. 366–385, 2014.
- [24] M. S. Omar, M. A. Anjum, S. A. Hassan, H. Parveiz, Q. Ni, “Performance Analysis of Hybrid 5G Cellular Networks Exploiting mmWave Capabilities in Suburban Areas”, *IEEE International Conference on Communications (ICC)*, May, 2016, Kuala Lumpur Malaysia.
- [25] S. A. R. Naqvi, S. A. Hassan, Z. Mulk, “Pilot Reuse and Sum Rate Analysis of mmWave and UHF-based Massive MIMO Systems”, *Pro-*

- ceedings of the IEEE Vehicular Technology Conference (VTC-Spring)*, May, 2016, Nanjing, China.
- [26] C. Li, J. Zhang, M. Haenggi, and K. B. Letaief, “User-centric intercell interference nulling for downlink small cell networks,” *IEEE Tran. on Commun.*, vol. 63, no. 4, pp. 1419–1431, 2015.
- [27] Z. Lu, T. Lei, X. Wen, L. Wang, and X. Chen, “SDN based user-centric framework for heterogeneous wireless networks,” *Mobile Information Systems*, vol. 2016, 2016.
- [28] G. P. Koudouridis, P. Soldati, H. Lundqvist, and C. Qvarfordt, “User-centric scheduled ultra-dense radio access networks,” *IEEE International Conf. on Telecommunications (ICT)*, pp. 1–7, 2016.
- [29] S. E. Elayoubi, E. Altman, M. Haddad, and Z. Altman, “A hybrid decision approach for the association problem in heterogeneous networks,” *IEEE INFOCOM*, pp. 1–5, 2010.
- [30] J. Andrews, S. Singh, Q. Ye, X. Lin, and H. Dhillon, “An overview of load balancing in HetNets: Old myths and open problems,” *IEEE Transactions on Wireless Communications*, vol. 21, no. 2, pp. 18–25, Apr. 2014
- [31] Q. Ye, B. Rong, Y. Chen, M. Al-Shalash, C. Caramanis, and J. Andrews, “User association for load balancing in heterogeneous cellular networks,” *IEEE Transactions on Wireless Communications*, vol. 12, no. 6, pp. 2706–2716, Jun. 2013.

- [32] Y. Wang, S. Chen, H. Ji, and H. Zhang, "Load-aware dynamic biasing cell association in small cell networks," *IEEE International Conference on Communications (ICC)*, pp. 2684–2689, Jun. 2014,
- [33] H. Klessig, M. Günzel, and G. Fettweis, "Increasing the capacity of large-scale HetNets through centralized dynamic data offloading," *IEEE 80th Vehicular Technology Conference (VTC)*, Sep.2014.
- [34] H. Inaltekin, M. Chiang, H. V. Poor, and S. B. Wicker, "On unbounded path-loss models: Effect of singularity on wireless network performance," *IEEE Journal on Selected Areas in Communications*, vol. 27, no. 7, pp. 1078–1092, Sep. 2009.
- [35] B. Romanous, N. Bitar, A. Imran, and H. Refai, "Network densification: Challenges and opportunities in enabling 5G," *IEEE International Workshop on Computer Aided Modelling and Design of Communication Links and Networks (CAMAD)*, pp. 129–134, 2015.
- [36] J. G. Andrews, "Seven ways that HetNets are a cellular paradigm shift," *IEEE Communications Magazine*, vol. 51, no. 3, pp. 136–144, Mar. 2013.
- [37] Z. Gao, L. Dai, D. Mi, Z. Wang, M. A. Imran, and M. Z. Shakir, "Mmwave massive-mimo-based wireless backhaul for the 5G ultra-dense network," *IEEE Wireless Commun.*, vol. 22, no. 5, pp. 13–21, 2015.
- [38] M. J. Feuerstein, K. L. Blackard, T. S. Rappaport, S. Y. Seidel, and H. Xia, "Path loss, delay spread, and outage models as functions of antenna height for microcellular system design," *IEEE Transactions on Vehicular Technology*, vol. 43, no. 3, pp. 487–498, Aug 1994.

- [39] D. Akerberg, “Properties of a TDMA pico cellular office communication system”, *IEEE Vehicular Technology Conference*, pp. 186–91, May 1989.
- [40] S. Hur et al., “Proposal on mmwave channel modeling for 5G cellular system,” *IEEE Journal of Selected Topics in Signal Processing*, June 2015.
- [41] X. Zhang and J. Andrews, “Downlink cellular network analysis with multi-slope path loss models,” *IEEE Trans. on Commun.*, vol. 63, no. 5, pp. 1881–1894, May 2015.
- [42] M. Ding, P. Wang, D. L’opez-P’erez, G. Mao, and Z. Lin, “Performance impact of los and nlos transmissions in small cell networks,” *IEEE Trans. Wireless Commun.*, Mar 2015.
- [43] N. Garg, S. Singh, and J. Andrews, “Impact of dual slope path loss on user association in hetnets”, *IEEE Globecom Workshops*, pp. 1–6, 2015.
- [44] P. Xia, V. Chandrasekhar, and J. G. Andrews, “Open vs. closed access femtocells in the uplink,” *IEEE Trans. Wireless Commun.*, vol. 9, no. 12, pp. 3798–3809, 2010.
- [45] Z. Hasan, H. Boostanimehr, and V. K. Bhargava, “Green cellular networks: A survey, some research issues and challenges,” *IEEE Commun. surveys & tutorials*, vol. 13, no. 4, pp. 524–540, 2011
- [46] S. Navaratnarajah, A. Saeed, M. Dianati, and M. A. Imran, “Energy efficiency in heterogeneous wireless access networks,” *IEEE wireless commun.*, vol. 20, no. 5, pp. 37–43, 2013.

- [47] X. Zhang, R. Yu, Y. Zhang, Y. Gao, M. Im, L. G. Cuthbert, and W. Wang, “Energy-efficient multimedia transmissions through base station cooperation over heterogeneous cellular networks exploiting user behavior,” *IEEE Wireless Commun.*, vol. 21, no. 4, pp. 54–61, 2014.
- [48] Z. Wang and W. Zhang, “A separation architecture for achieving energy-efficient cellular networking,” *IEEE Trans. Wireless Commun.*, vol. 13, no. 6, pp. 3113–3123, Jun. 2014.
- [49] T. Basar, G. J. Olsder, G. Olsder, T. Basar, T. Basar, and G. J. Olsder, “Dynamic Noncooperative Game Theory,” 2nd ed. Philadelphia, PA: SIAM, 1999.
- [50] S. Sun et al., “Path loss, shadow fading, and line-of-sight probability models for 5G urban macro-cellular scenarios,” *IEEE Global Communications Conference, Exhibition and Industry Forum (GLOBECOM) Workshop*, Dec. 2015.